INVITED PAPER

A Novel Framework for the Design of Change-Detection Systems for Very-High-Resolution Remote Sensing Images

In this paper, change detection in multitemporal VHR images is discussed. A framework is proposed that aims at defining a top–down approach to the design of novel change-detection systems for multitemporal VHR images.

By Lorenzo Bruzzone, *Fellow IEEE*, and Francesca Bovolo, *Member IEEE*

ABSTRACT | This paper addresses change detection in multitemporal remote sensing images. After a review of the main techniques developed in remote sensing for the analysis of multitemporal data, the attention is focused on the challenging problem of change detection in very-high-resolution (VHR) multispectral images. In this context, we propose a framework that aims at defining a top–down approach to the design of the architecture of novel change-detection systems for multitemporal VHR images. The proposed framework explicitly models the presence of different radiometric changes on the basis of the properties of multitemporal images, extracts the semantic meaning of radiometric changes, identifies changes of interest with strategies designed on the basis of the specific application, and takes advantage of the intrinsic multiscale/multilevel properties of the objects and the high spatial correlation between pixels in a neighborhood. This framework defines guidelines for the development of a new generation of change-detection methods that can properly analyze multitemporal VHR images taking into account the intrinsic complexity associated with these data. In order to illustrate the use of the proposed framework, a real change-detection problem has been considered, which is described by a pair of VHR multispectral images acquired by the QuickBird satellite on the city of Trento, Italy. The proposed framework has been used for defining a system for change detection in the two images. Experimental results confirm the effectiveness of the developed system and the usefulness of the proposed framework.

KEYWORDS | Change detection; image processing; multitemporal images; remote sensing; very high geometrical resolution images

I. INTRODUCTION

In remote sensing, change detection is the process that leads to the identification of changes occurred on the Earth surface by jointly processing two (or more) images acquired on the same geographical area at different times. Thanks to the repeat-pass nature of satellite orbits, remote sensing images can be acquired regularly over a given target area. Thus, they become an ideal information source for performing automatic change detection.

In the last decade, a new generation of satellite sensors has been operated, which can acquire panchromatic (PAN) and/or multispectral (MS) images with submetric and metric resolution. Among these satellites, we recall WorldView-1 and -2, Ikonos, Eros, QuickBird, SPOT-5, etc. From 2007, it is also possible to acquire satellite synthetic aperture

Manuscript received December 23, 2011; revised April 6, 2012; accepted April 7, 2012. Date of publication July 24, 2012; date of current version February 14, 2013. This work was supported by a project founded by the "Provincia Autonoma di Trento" (Autonomous Province of Trento).

The authors are with the Department of Information Engineering and Computer Science, University of Trento, Povo, Trento I-38123, Italy (e-mail: lorenzo.bruzzone@ing.unitn.it; francesca.bovolo@disi.unitn.it).

Digital Object Identifier: 10.1109/JPROC.2012.2197169

radar (SAR) images with resolution up to 1 m, thanks to the COSMO-SkyMed constellation and the TerraSAR-X and Tandem-X missions. In this paper, we will refer to such data as very-high-resolution (VHR) images. From a general perspective, VHR multitemporal images represent a valuable and rich information source for performing the detection of changes occurred on the Earth surface. However, the huge amount of data acquired from the satellite sensors requires the definition of automatic and unsupervised change-detection methods that can extract the change information without relying on both the manual processing of experts and the availability of ground truth information. Although effective methods exist for the analysis of moderate (i.e., hundreds of meters, like MODIS data) and high (i.e., tens of meters, like Landsat Thematic Mapper data) resolution multitemporal images [1]–[4], at the present, the situation is different for VHR images with metric or submetric resolution [5]. In such images, the increased geometrical resolution results in the possibility of identifying much more details. Thus, VHR images are more heterogeneous and the definition of the change-detection task becomes more complex. In order to better understand the complexity of change detection in VHR images, it is interesting to focus the attention on the concept of change in a more general context.

The complexity associated with the concept of change in a heterogeneous scenario has long been known and is widely investigated and documented in the perception and psychology literature [6], [7]. Here we recall some relevant concepts. Let us consider an observer that has to detect changes in daily life scenarios. Such a task is highly complex mainly because the definition of change in a structured scenario is intrinsically complex and subjective. For human observers the accuracy in change detection depends on the magnitude of the change and on which property of objects has changed (e.g., presence/absence, orientation, size, shape, color, semantic identity). Some events (e.g., new objects in the scene) may be easier to detect than others (e.g., change in orientation). The human ability in detecting changes depends on both the perceptual salience and the semantic relevance of the change to the observer itself (changes might be relevant to somebody and not relevant to somebody else). In the literature, the most commonly cited example is the one related to the ability in detecting changes in football games. Football experts will be faster and more efficient in detecting changes rather than nonexperts. Thus, in general, an observer better detects changes for which he/she has a high-level knowledge, whereas he/she tends to fail for the others [6]. A similar reasoning can be applied if we consider software-based (semi)automatic change-detection approaches. Thus, even if change detection is a process addressed in many research fields (e.g., data stream analysis [8], image processing [1], remote sensing [2], [9], video processing [10], automotive [11], neuroscience [12], medical treatment [13]), most of the techniques developed for an application domain may not effectively work on a different domain (i.e., they have been developed using high-level knowledge associated with the specific application). Thus, a method (as well as an observer) detects better changes with specific semantic meaning than others.

When considering VHR remote sensing images, the change-detection problem shares many of the observations listed above. This is a very complex task because the high information content of VHR images requires an accurate definition and modeling of the concept of change (which is often associated with the specific goal of the application) and thus the development of techniques that can detect changes according to this definition. Moreover, the complexity is increased by the need to take into account all the specific issues related to the properties of VHR remote sensing images. Standard unsupervised change-detection techniques presented in the remote sensing literature are often not based on a detailed analysis of the concept of change. Usually they compare two images acquired on the same geographical area at different times by assuming that their radiometric properties are similar except for the presence of changes occurred on the ground. Unfortunately, this assumption is seldom satisfied, especially in VHR images [14]. This is due to both the complexity of the objects present in the scene (which may show different spectral behaviors at two different dates even if their semantic meaning does not change) and differences in the acquisition conditions (e.g., sensor acquisition geometry, atmospheric and sunlight conditions). These factors strongly affect images taken at metric or submetric resolution and thus the change-detection process. In order to reduce the impact of all the mentioned factors, it is not sufficient to apply radiometric and geometric corrections to the images and then extract radiometric changes, but it becomes mandatory to analyze the semantic meaning of each kind of radiometric change. In order to identify the semantic meaning of each radiometric change, it is necessary to define techniques being able to extract the information in multitemporal data at different abstraction levels. These levels should be effectively combined according to strategies designed for the specific application, i.e., taking into account the specific kind(s) of change relevant for end users. It is worth noting that, even if some change-detection techniques for VHR images have been proposed in the literature, in most of the cases, they are focused on specific applications (e.g., landslides [15], damaged-building mapping [16]) and do not address the problem from a general perspective. Moreover, in many cases, these methods model the spatial context of pixels or the multiscale properties of objects, but neglect the key problem of the distinction between radiometric and semantic changes. This is a serious limitation for a successful change-detection process in VHR images.

In this paper, we address the aforementioned issues by analyzing the main properties of the problem of change

detection in VHR multitemporal images and by proposing a general framework and precise guidelines for defining effective change-detection approaches. In order to achieve these goals, we first define the taxonomy of causes versus semantic meaning that can be associated with radiometric changes in VHR remote sensing images. This taxonomy is fundamental for identifying and modeling in a precise way different sources of radiometric changes expected in a given change-detection problem. Then, we propose two strategies (i.e., a direct approach and an approach by cancellation) to the design of change-detection methods. Both strategies take advantage of the aforementioned taxonomy as well as of abstraction levels for effectively modeling and extracting the semantic of radiometric changes from multitemporal data. We will show that multiscale information can be extracted in change detection according to a bidirectional structure (depending on the available information about the problem) for either computing high abstraction levels (meta-levels) given the original multitemporal data (simplification process) or deriving lower abstraction levels given higher ones (prediction process). Such an approach also becomes highly useful when multisensor or multisource data sets are considered as the use of both simplification and prediction allows one to define meta-levels where information acquired by different sources at different times can be compared.

The proposed framework is illustrated in the solution of a complex real change-detection problem described by a pair of multitemporal multispectral QuickBird VHR images. The data set represents a case with different kinds of radiometric changes that depend on the acquisition system and are not of interest of end users. The change-detection architecture and the related algorithms are designed on the basis of the proposed framework. The change-detection system isolates the different sources of radiometric change and generates the change-detection map including only changes relevant to the application, neglecting the others. The final results demonstrate the effectiveness of the proposed system and the usefulness of the framework.

The rest of the manuscript is organized into six sections. Section II presents an analysis of the state of the art on change detection in multispectral images. Section III gives an overview of the proposed framework for change detection in VHR images. Section IV describes the taxonomy of radiometric changes and the general procedure for defining the tree of radiometric changes used in the next phases of the framework. Section V illustrates the proposed approaches to both the construction of effective change-detection architectures and the extraction of the multiscale information in multispectral images. Section VI presents the application of the proposed framework to a real change-detection problem. Finally, Section VII draws the conclusion of this work.

II. OVERVIEW ON CHANGE-DETECTION TECHNIQUES FOR MULTISPECTRAL REMOTE SENSING IMAGES

In the last 30 years, the remote sensing community has devoted large attention to automatic change-detection techniques. Extensive overviews on this topic can be found in [1]–[4]. Despite the fact that much effort has been put in the development of effective change-detection techniques, the problem is challenging and additional work is still needed for defining new and more efficient methods. This is mainly due to the availability of the aforementioned images acquired by the last generation of satellite sensors that show a higher spatial resolution (less than 1 m) than old generation images. The increased resolution makes the state-of-the-art change-detection methods less effective on new data. Moreover, new data properties allow one to develop novel applications that could not be faced before. Thus, there is a strong need for the definition of new change-detection methods being able to properly handle the high amount of spatial information in new generation data.

In the literature, many approaches have been developed to detect changes in multitemporal images for both multispectral and SAR remote sensing images. In this work, the attention is mainly devoted to multispectral images. The approaches to change detection can be essentially divided into two groups: 1) supervised [3], [5], [14], [15], [17]–[26]; and 2) unsupervised approaches [27]–[37]. The former group includes methods that require ground reference information as they are based on the use of supervised classifiers. This information can be required for all available acquisitions, or only for one of them (e.g., when semisupervised and domain adaptation methods are considered [25], [26], [38]). This ground reference information can be retrieved with *in situ* campaigns, by photointerpretation or from prior knowledge on the scene. Collection of reference data has an associated cost in terms of time and effort, which in multitemporal data processing should be multiplied by the number of images for which such information is required. Thus, considering that the number of potential temporal acquisitions on a given area can be high, supervised methods are becoming less appealing from the application point of view. On the contrary, unsupervised methods do not need any ground reference data for producing the change-detection map and thus are more attractive from the operational viewpoint. These methods can mainly give information about presence/absence of changes [28], [29], [31], [39] and only in specific cases about the presence of different kinds of changes [27], [40]. However, they cannot explicitly identify the exact land-cover transition associated with the change since ground reference information is not available.

When dealing with unsupervised change detection, preprocessing of multitemporal images becomes highly important because most of the approaches suffer of

differences in image radiometry and/or geometry. In the literature, studies exist on the effects of residual misregistration on the change-detection results [41]–[43], and techniques devoted to mitigate these effects (and thus change-detection errors associated to them) have been proposed [14], [44], [45]. Other papers are devoted to the analysis of effects of pan-sharpening algorithms [46] and radiometric differences [27], [47]–[49] on the change-detection process.

Many unsupervised methods are pixel based [29], [31], [33], [40], [50] and focus on the analysis of the characteristics of the multispectral difference image obtained by pixel-by-pixel subtraction of multispectral images. Most of them compute the magnitude of change vectors associated with the multispectral difference image and apply thresholding techniques to it in order to separate changed from unchanged pixels [29], [31]. These methods are intrinsically unable to identify possible different kinds of change. In order to overcome this drawback, more recently developed methods also consider the direction of spectral change vectors in the change-detection process associating to different kinds of change clusters of pixels having different direction [27], [40]. Other groups of pixel-based approaches to change detection are defined by using: 1) fuzzy set theory [51]–[59]; 2) data-driven transformations (e.g., principal component analysis [37], independent component analysis [60], multivariate alteration detection [36], [61], [62]); and 3) similarity measures [63]. All these methods demonstrated their effectiveness on moderate and high geometrical resolution images (from tens to hundreds of meters of spatial resolution) and in several applications. However, when the geometrical resolution of images increases up to less than 1 m, they become less accurate. This is mainly due to the fact that most of them assume that spatially adjacent pixels are independent from each other (with the exception of methods based on canonical correlation analysis that are less sensitive to spatial correlation among pixels [64]). Despite the fact that this is an acceptable assumption for moderate/high spatial resolution data, it is not for images that exhibit very high spatial resolution. Accordingly, in the last years, novel approaches have been developed which take into account the dependence between spatially adjacent pixels as well as the multiscale information in the images. Spatial-context information can be modeled by: fixed-shape neighborhood systems for texture information extraction [65]–[67], applying Markov random fields theory [31], [35], or using morphological filters [32], [68]. More advanced methods perform a context-sensitive analysis by considering adaptive neighborhoods modeled by multitemporal parcels [5], [30], [69] and object properties [15], [16], [20], [70]–[73]. They better capture the spatial correlation information present in the scene and become particularly promising for VHR images showing complex objects (e.g., buildings and other man-made structures). In order to effectively model objects in the images at different scales, some of the concepts employed in the previously mentioned papers such as morphological filters, multitemporal parcels, and even Markov random fields can be adapted and used in multiscale/multilevel analysis [5], [32], [35], [68], [74], together with specific multiscale/multilevel representation tools such as wavelet transform [39], [75], [76].

As is clear from this analysis, many techniques have been developed for addressing specific change-detection problems under different basic assumptions. However, many open issues still need to be addressed, especially when considering VHR images. In order to address the change detection problem in a more structured (and thus effective) way, in the following sections, we define a framework for the definition of new change-detection architectures, which is developed taking into account the properties of VHR images.

III. PROPOSED FRAMEWORK FOR THE DEFINITION OF CHANGE-DETECTION ARCHITECTURES FOR VHR IMAGES

The proposed framework for the design of change-detection architectures for VHR multitemporal images is described by the flowchart shown in Fig. 1. The idea is that starting from the specific properties of the problem we can design the architecture of an effective change-detection system following a top–down approach. Once the general architecture is defined, its elements can be implemented with specific data analysis techniques in order to derive the final change-detection system. In this way, it is possible to design structured systems that properly model the complexity of the change-detection problem based on a relatively simple strategy with a set of well-defined guidelines.

The proposed framework is based on three main components.

1) Identification and modeling of the expected kinds of radiometric changes occurred between the images and definition of the *tree of radiometric changes*. This requires an *a priori* understanding of the possible causes of radiometric changes between multitemporal VHR images and an analysis of their impact on the specific problem. The goal is to limit errors due to sources of change that are not of interest of the application and can be predicted.
2) Definition of a change detection architecture based on the tree of radiometric changes that describes the problem. The architecture can be based either on a direct extraction of the radiometric changes of interest or on a detection by cancellation of noninteresting radiometric changes.
3) Extraction of the semantic from radiometric changes according to multilevel and hierarchical

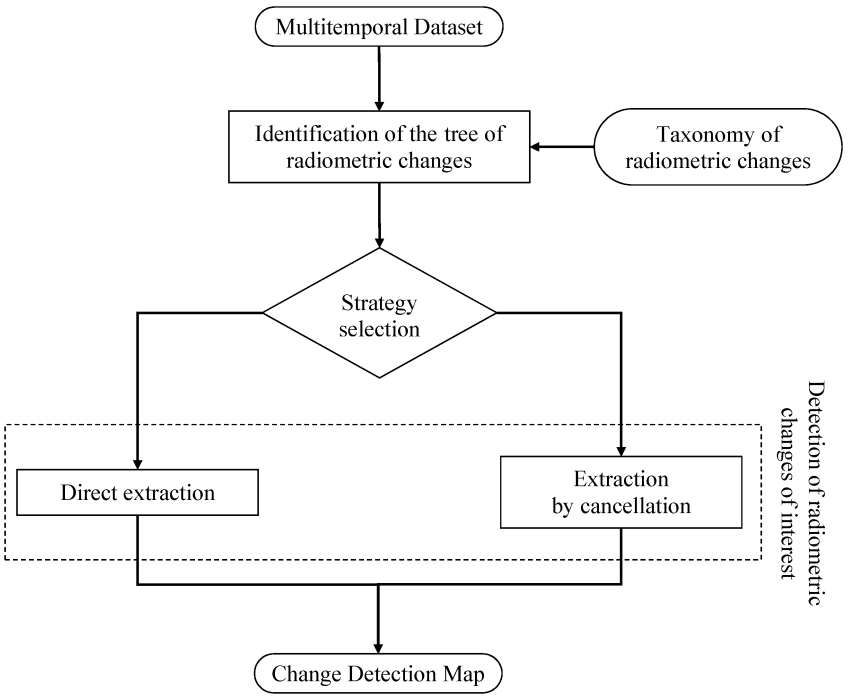

Fig. 1. *Flowchart of the proposed procedure for the definition of novel change-detection methods.*

techniques. This is the phase in which the data analysis techniques associated with the different blocks of the change-detection architecture are designed for extracting the semantic of radiometric changes.

The proposed framework is devised for remote sensing VHR multitemporal images. However, the general concepts can be also applied to the design of change-detection techniques in other research fields. The design of change-detection architectures has to be performed offline in cooperation with the end users. The precise definition of which kinds of change are of interest for end users results in high-level knowledge that can be used for extracting changes having the expected semantic. Thus, prior knowledge significantly reduces the sources of errors. Once the design and the setup of the architecture are over, the resulting system can be automatic or semiautomatic depending on the techniques adopted for implementing parts of the architecture. In the following, we will describe in greater details the main components of the proposed framework.

IV. IDENTIFICATION AND MODELING OF RADIOMETRIC CHANGES

The first step of the proposed architecture requires the identification and modeling of radiometric changes. To this end, a categorization of the different kinds of radiometric changes that can be present in a multitemporal data set is necessary. In the following, we propose a taxonomy of radiometric changes which has a general validity in natural environments, but is particularly suitable for VHR optical remote sensing images. Based on this taxonomy, different sources of radiometric changes can be connected to the different kinds of change. The explicit cause–effect relationship represents the high-level knowledge that guides the definition of methodologies for detecting and isolating radiometric changes relevant to end users from all the others. In Section IV-A and B, we first describe the general taxonomy of radiometric changes and then propose a procedure for building the tree of radiometric changes given a specific application.

A. Taxonomy of Radiometric Changes

A basic component for the development of a change-detection algorithm is the taxonomy that relates radiometric changes that can occur between multitemporal VHR images with their semantic meaning. This is propaedeutic to identify and model the different kinds of radiometric changes present in the considered problem and data set.

The high complexity of VHR images mainly depends on two sets of factors: 1) the intrinsic geometrical complexity, the spectral nonhomogeneity, and the multiscale properties of the objects; and 2) possible different acquisition conditions of multitemporal data. The first set of factors is

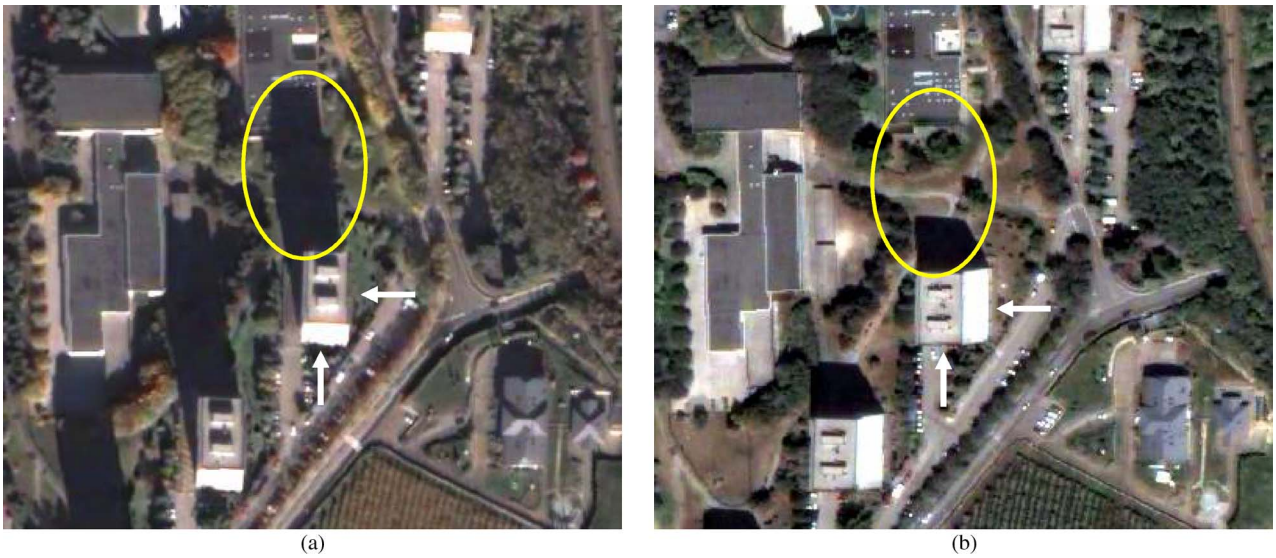

Fig. 2. *Multitemporal image pair showing the effect of acquisition conditions in terms of acquisition sensor view angle and sun incidence angle. Images were taken from the QuickBird VHR sensor over the city of Trento, Italy, in: (a) October 2005 and (b) July 2006.*

associated with the complexity of the objects imaged at metric or submetric resolution. Objects homogeneous from a semantic viewpoint (e.g., buildings) have often spectral signatures that, at very high resolution, result inhomogeneous due to the different subobjects from which they are composed (e.g., a building roof may be composed of different pitches, vegetation, chimneys). The second set of factors is crucial because it makes it complex a proper comparison between multitemporal data. For example, different sensor view angles imply differences in the acquisition geometry and in shadows resulting in significantly different object representations in the acquired images. In addition, in optical images, differences due to seasonal effects and illumination conditions sharply modify spectral signatures.

All the aforementioned issues, when projected on the comparison of multitemporal images, result in a large set of possible radiometric changes having significantly different semantic meaning. The semantic meaning (which is associated to the cause of the change itself) should guide the definition of the change-detection strategy. Fig. 2 shows a simple example with a pair of VHR images acquired over the city of Trento, Italy, in October 2005 and July 2006 by the QuickBird satellite. The two images look quite different due to the problems listed above. As an example, acquisition season (shadows in yellow circles in Fig. 2) and sensor view angle (white arrows in Fig. 2) affect the building in the center of the image. A pixel-based automatic change-detection approach would highlight such area as being changed since it is affected by strong radiometric variations. However, the building did not change between the two acquisitions. Thus, a user looking for changes in urban areas would not like to see this building (and its surroundings) highlighted in the final change-detection map.

Radiometric changes (Ω_{Rad}), even if associated with different sources, may exhibit characteristics similar to each other. Thus, in order to separate kinds of radiometric changes from each other, it is necessary to explicitly extract their semantic meaning. This requires an analysis of their cause(s) and a proper data-processing approach. At the highest level, we can distinguish between radiometric changes due to: 1) acquisition conditions (Ω_{Acq}); and 2) changes occurred on the ground (Ω_{Grd}). Thus, the set of radiometric changes can be modeled as $\Omega_{\text{Rad}} = \{\Omega_{\text{Acq}}, \Omega_{\text{Grd}}\}$. Each category can be detailed in subcategories (Fig. 3 summarizes the outcomes of this analysis).

Changes due to acquisition conditions (Ω_{Acq}): this kind of radiometric changes is essentially related to differences in 1) the atmospheric conditions at the acquisition dates (Ω_{Atm}), and 2) the acquisition system (Ω_{Sys}). Accordingly, we can write

$$\Omega_{\text{Acq}} = \{\Omega_{\text{Atm}}, \Omega_{\text{Sys}}\}. \quad (1)$$

Differences in atmospheric conditions (Ω_{Atm}) mainly affect passive sensor images. They are due to changes in weather conditions causing the presence/absence of clouds and/or variations in the atmospheric transmittance [Fig. 4(a)]. The latter ones can be mitigated in the preprocessing with methods for atmospheric corrections, whereas clouds should be extracted at a higher level of processing with proper cloud-detection algorithms [77], [78].

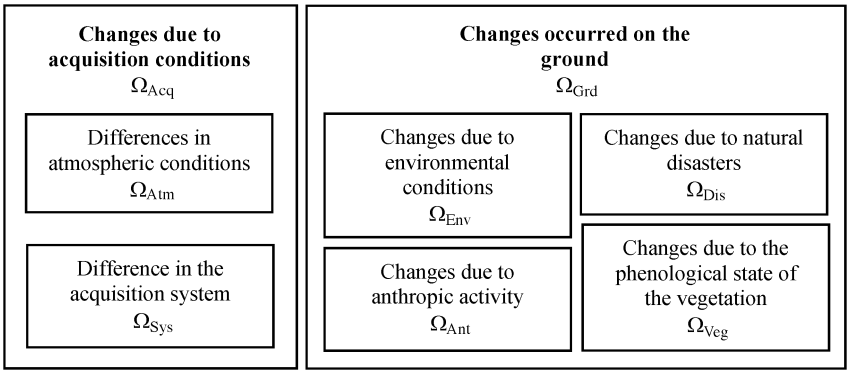

Fig. 3. *Taxonomy of the causes of radiometric changes in VHR images.*

Differences in the acquisition system (Ω_{Sys}) are related to changes in: 1) the acquisition sensor type; 2) the acquisition mode of the sensor; 3) seasonal effects (like the incidence angle of the solar rays); and 4) the view angle of the sensor (which is a very important variable in VHR images as it can be changed in different acquisitions) [Fig. 4(b)].

The aforementioned differences, even after preprocessing, induce a set of radiometric changes associated with: 1) differences in cloud cover; 2) differences in shadows; 3) different portions of the same object imaged with different view angles; and 4) residual misalignment in border regions between objects due to geometric differences (registration noise). This set of radiometric changes should be identified in the change-detection architecture and removed from the final change-detection map as they are not relevant from the perspective of the end user.

Changes occurred on the ground (Ω_{Grd}) are the changes commonly relevant from the user's point of view. Nonetheless, there are many possible changes that may occur on the ground and can affect the sensor measurements. In this paper, we propose a possible general categorization that, however, cannot be exhaustive or complete, as subjective criteria could be used for defining categories. Changes occurred on the ground may be due to: 1) the phenological state of the vegetation (Ω_{Veg}); 2) the environmental conditions (Ω_{Env}); 3) the effects of natural disasters (Ω_{Dis}); and 4) the anthropic activity (Ω_{Ant}). Thus, we can write

$$\Omega_{Grd} = \{\Omega_{Veg}, \Omega_{Env}, \Omega_{Dis}, \Omega_{Ant}\}. \quad (2)$$

Changes due to the phenological state of the vegetation (Ω_{Veg}) are due to the season turnover that may result in sharp radiometric differences. Examples of such kind of changes are: the fall of the leaves which modify both the tree reflectance as well as the reflectance of the terrain on which the leaves fall, the change in the state (and thus in the spectral signature) of vegetation, etc. [Fig. 5(a)]. In order to limit the effects of this kind of changes, it would be necessary to consider images acquired in the same acquisition condition (i.e., in the same season). However, this constraint cannot be satisfied in all applications and the implication of a nonoptimal choice should be considered and modeled.

Changes due to the environmental conditions (Ω_{Env}) may induce long- or short-term radiometric changes. Long-term changes are mainly associated with climate changes due, for examples, to changes in the average temperature (e.g., desertification process, glaciers reduction). Short-term changes are, for example, changes in the soil

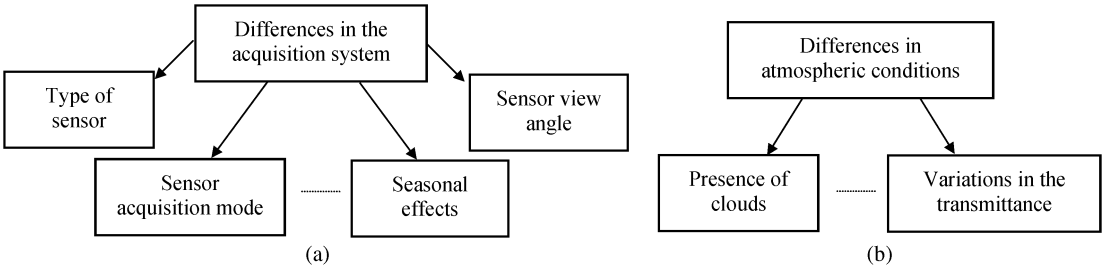

Fig. 4. *Taxonomy of the causes of radiometric changes due to differences in the acquisition conditions: (a) causes related to the acquisition system; and (b) causes related to atmospheric conditions.*

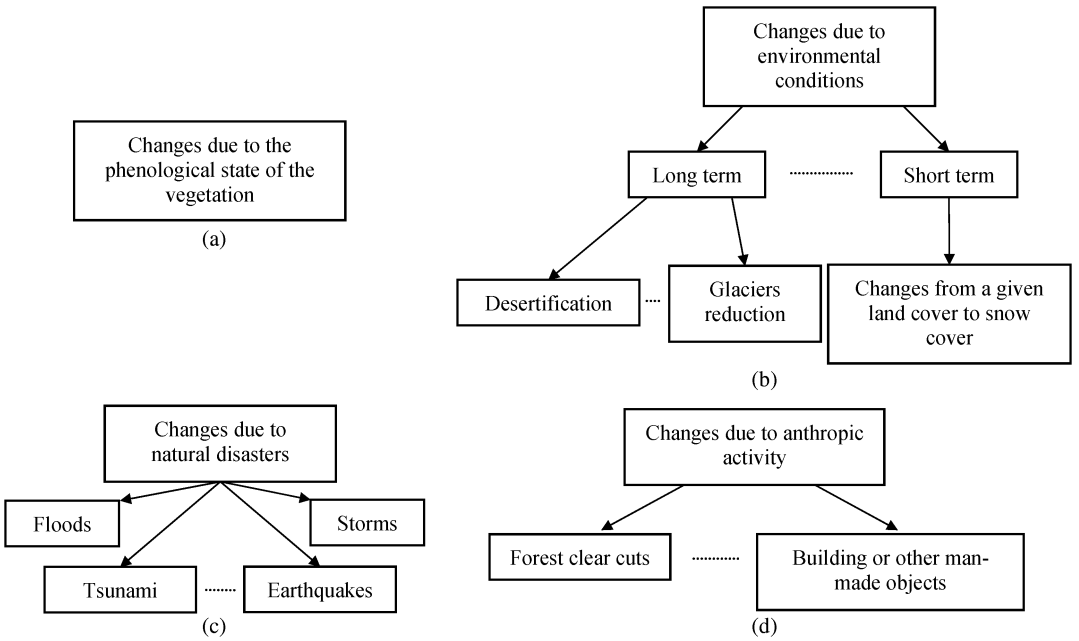

Fig. 5. *Taxonomy of the causes of changes occurred on the ground: (a) changes due to phenological state of the vegetation; (b) changes due to environmental conditions; (c) changes due to natural disasters; and (d) changes due to anthropic activity.*

moisture, changes from a given land cover to snow cover, etc. [Fig. 5(b)].

The detection of such kind of changes is relevant in the field of environmental monitoring. As an example, variations in soil moisture content represent a significant input for the analysis of the irrigation process, the agricultural management, etc. Another example is related to changes in the snow cover that become an input for the analysis of avalanche and flood risk [79]. Nonetheless, these changes may be a source of noise when the goal is to detect changes related, for instance, to anthropic activity.

Changes due to natural disasters (Ω_{Dis}) are associated with events like floods, earthquakes, tsunami, storms, forest fires, etc. [Fig. 5(c)]. They generate abrupt changes in the land cover. Detecting such kind of changes becomes of high importance for emergency response and damage assessment, and represents one of the most important applications of change detection. The use of VHR images for identifying damages caused by natural disasters is particularly important for a detailed evaluation of the effects of such disasters [73], [80]–[83].

Changes due to anthropic activity (Ω_{Ant}) reflect the effects of human activity that may induce many different kinds of land-cover changes. These changes can be related to forest clear cut, new buildings, or other man-made objects, etc. [Fig. 5(d)]. When dealing with VHR images usually the latter are very interesting from the application viewpoint as they are not detectable in images with moderate or high spatial resolution [5], [14].

All mentioned causes of change can result in statistically significant variations of the radiance in corresponding pixels (or objects). Depending on the application, some of them may be of interest to the end user, whereas others may not. However, in the literature, few unsupervised approaches exist that try to separate the different sources of change in a structured way [84], [85]. Most of the methods handle problems related to a specific application without a proper modeling of all the aforementioned causes of change. Therefore, there is a need of defining an approach that gives explicit guidelines for the separation of sources of change.

B. Definition of the Tree of Radiometric Changes

From the above taxonomy, it is clear that the generation of an accurate change-detection map, where only changes relevant to the application should be identified, implies the distinction between different sources of radiometric changes. The described taxonomy is general and represents the main kinds of radiometric changes that can be present in multitemporal VHR images. Given a specific problem, this taxonomy should be specialized on the application and data sets, i.e., *the tree of radiometric changes* associated with the problem should be defined. This tree is of fundamental importance for the next steps, as it models all the radiometric changes and their cause–effect relationships. The tree of radiometric changes can be defined as the result of the analysis of the considered problem and data set on the basis of the taxonomy defined in Section IV-A. The goal is to build a tree that identifies all the radiometric changes expected in the problem, including both the undesired changes due to the acquisition system and the changes occurred on the

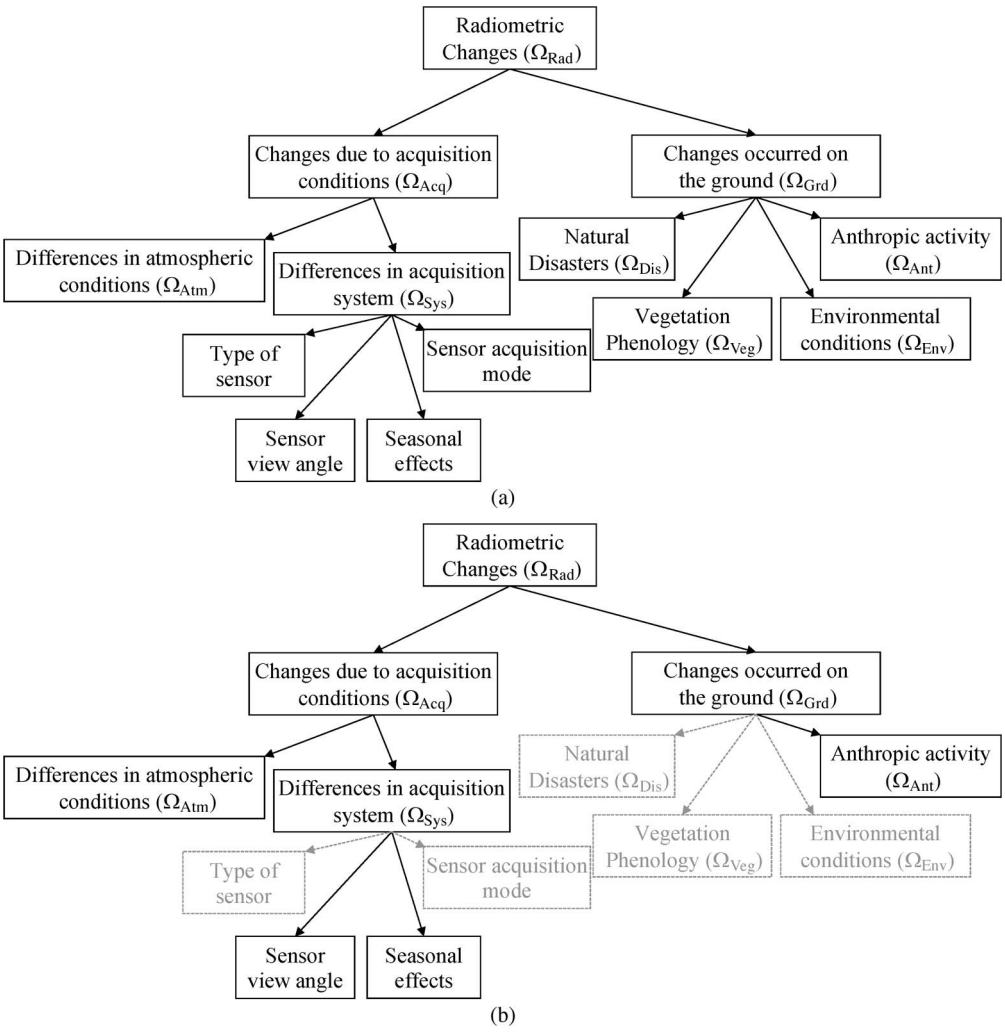

Fig. 6. ***Example of tree of radiometric changes: (a) general tree; and (b) pruned tree defined for a specific application (light-gray dashed elements are the pruned ones).***

ground [Fig. 6(a)]. Then, one can decide if all of them are of interest, or if some may be of interest (e.g., changes associated with buildings) and others may not (e.g., changes due to the vegetation phenology). In the first case, the design of the change-detection architecture can be done by considering a pruned version of the tree of radiometric changes [Fig. 6(b)], where leaves associated with kinds of changes occurred on the ground do not need to be modeled anymore. In the second case, all the leaves should be modeled in order to effectively discriminate changes of interest from the others.

V. DETECTION OF THE RADIOMETRIC CHANGES OF INTEREST

The aforementioned definition of the problem results in the need of defining multilevel-change-detection approaches, which can both: 1) model sources of radiometric changes present in the data and extract them from the images; and 2) take into account the intrinsic multiscale nature of objects present in VHR images. This allows one to simplify the distinction between relevant changes and nonrelevant ones (which becomes in turn source of errors). In this section, we describe both: 1) possible architectures for extracting radiometric changes of interest; and 2) multiscale strategies for extracting the semantic meaning of different radiometric changes present in VHR images.

A. Architectures for Detecting Radiometric Changes of Interest

Let $\mathbf{X}_1$ and $\mathbf{X}_2$ be two VHR images acquired over the same geographical area at times t_1 and t_2. To solve the change-detection problem defined by them, two architectures can be adopted: 1) differential detection of radiometric changes of interest by cancellation of the changes

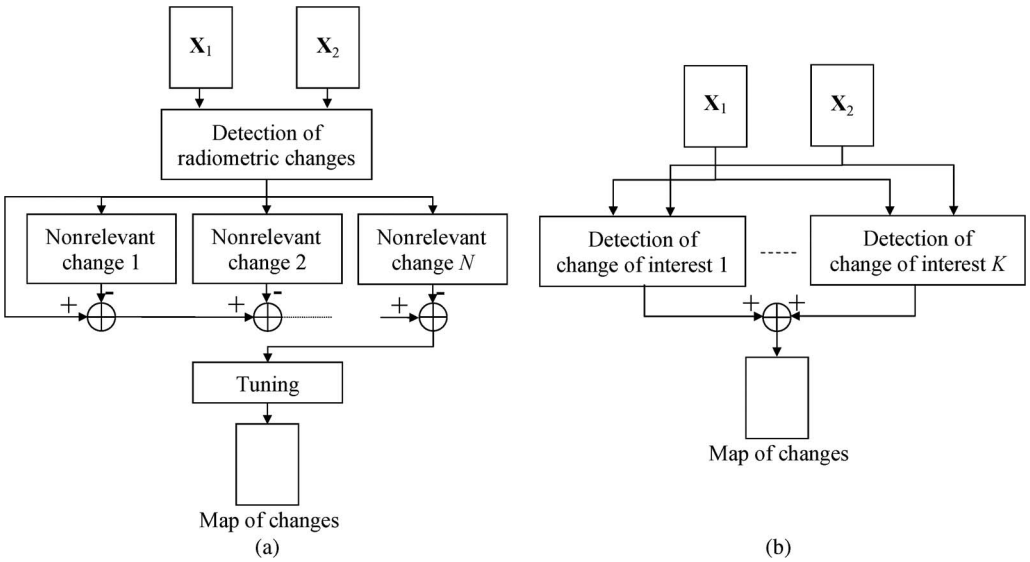

Fig. 7. ***Proposed architecture based on: (a) differential extraction of changes of interest by cancellation; and (b) direct extraction of changes of interest.***

due to acquisition conditions (e.g., residual registration noise, difference in shadows) and more in general nonrelevant from the end-user viewpoint [Fig. 7(a)]; and 2) direct extraction of the changes of interest (i.e., those with the desired semantic) [Fig. 7(b)]. Of course the two strategies can be integrated for optimizing the change-detection results.

The choice among strategies depends on the specific problem and on the availability of methods being able to extract the sources of radiometric changes from the data. In some cases, it is possible to directly focus the attention on changes of interest. In other cases, it is not possible (or difficult) to extract the changes of interest because their semantic cannot be derived directly from the analysis of the images. Thus, it is more effective to detect the radiometric changes that are not interesting, and remove them from the map of all radiometric changes. Once nonrelevant changes have been removed, a tuning step can be applied that refines the change-detection results on the basis of the properties of unchanged pixels and radiometrically changed pixels associated to relevant changes. The refinement step can be important to reduce misclassified pixels since the decision process is performed after reducing some sources of noise. This process will be better illustrated in the example described in the experimental part of this paper.

The fusion between kinds of radiometric changes (modeled for simplicity with the sum node in the architectures of Fig. 7) can be carried out according to three strategies: 1) pixel-based crisp strategies; 2) pixel-based fuzzy strategies; and 3) context-based strategies. The pixel-based crisp approach uses the binary maps of specific radiometric changes detected at the previous levels according to simple crisp rules based on the pixel-by-pixel label (change and no change) comparisons. The pixel-based fuzzy approach uses in comparison the indices that are obtained for modeling the radiometric changes of interest, before being analyzed (e.g., according to thresholding techniques) for generating a binary map. This may result in a better use and modeling of the available information and uncertainty with respect to crisp-based approaches. Finally, the context-based approach takes advantage of the spatial neighborhood of each pixel in the definition of the integration rule. The context-based fusion can be carried out by analyzing either crisp or fuzzy maps of radiometric changes. The analysis can be performed by defining fixed neighborhood or adaptive multitemporal regions. An example of context-based crisp fusion will be presented in the experimental part of this paper.

B. Extraction of the Semantic From Radiometric Changes

Due to the high complexity of VHR images, the identification of radiometric changes with different semantic meaning and/or associated with different sources of noise is a complex task. In general, to achieve this goal in VHR images, the comparison between multitemporal images should be performed at a conceptual level (meta-level) higher than that of simple pixel radiometry (i.e., pure pixel level) and should include more than one level in the process. This requires additional steps for the extraction of the semantic information. To this end, we introduce the concept of descriptor $D(.)$ as basic element of the change-detection process. A descriptor is any possible feature extracted from the image and can be modeled as a function of: the sensor (S), the acquisition condition (Acq), and the

ground conditions (Grd), i.e., $D(S, \mathrm{Acq}, \mathrm{Grd})$. It is worth recalling that, despite the fact that preprocessing can be applied to reduce the dependence from acquisition conditions, some effects cannot be fully controlled. Thus, they result in undesired radiometric changes.

Descriptors can be related to each single image of the pair to be analyzed (*single data descriptor*) or to both of them (*multitemporal descriptors*). They may represent features at different meta-levels of increasing abstraction such as: pixel level (px), primitive level (p), and object level (o). By increasing the abstraction level of the descriptor, the dependency from the sensor and the acquisition condition decreases, whereas the one with respect to the ground condition is preserved. The pixel level considers pixel radiometry, including multispectral channels acquired by the sensor (and thus the spectral signatures of the objects on the ground in multispectral images) and other pixel-based descriptors (e.g., vegetation indexes [4] and shadow indexes [86]). The primitive level is associated with geometric or statistical features that can be extracted from the multitemporal images. Examples of geometric primitives are lines, regions with specific size or shape extracted by segmentation, morphological filters [21], and attribute filters [68]. Examples of statistical primitives are parameters extracted on fixed or adaptive shape neighborhoods of pixels (e.g., mean, variance, skewness, kurtosis, and texture computed by the co-occurrence matrix [87]). The object level can be obtained by combining primitives in order to identify the semantic label of the instances and comparing them in multitemporal data.

Let us now formalize the previous concepts for defining all the main elements that should be considered. Let $\boldsymbol{D}_i = \{D_{i,j}^{px}, D_{i,j}^{p}, D_{i,j}^{o}\}$ represent a generic set of single date descriptors of the image acquired at time $i = \{1, 2\}$. Let $D_{i,j}^{px}$, $D_{i,j}^{p}$, $D_{i,j}^{o}$ be the jth ($j = 1, \ldots, J^k$ with $k = \{px, p, o\}$) descriptor of image $\mathbf{X}_i$ at pixel, primitive, and object levels, respectively. Thus, the information of a given image $\mathbf{X}_i$ can be represented by a set of descriptors $\boldsymbol{D}_i$ that model information at different meta-levels (from the pixel to higher semantic levels). In our notation, the first descriptor at pixel level $D_{i,1}^{px}$ corresponds to the image $\mathbf{X}_i$. Accordingly, $D_{i,1}^{px}$ is a function of S, Acq, and Grd, i.e., $D_{i,1}^{px}(S_i, \mathrm{Acq}_i, \mathrm{Grd}_i)$. Semantic descriptors at corresponding levels in $\boldsymbol{D}_i$ computed on different temporal images can be compared according to proper algebraic operators $\Delta_j^k(\cdot)$ for extracting multitemporal descriptors at different abstraction levels. The $\Delta_j^k(\cdot)$ operator is a function of both the descriptor k ($k = \{px, p, o\}$) and the specific feature j ($j = 1, \ldots, J^k$). It generates a set $\boldsymbol{D} = \{D_j^{px}, D_j^{p}, D_j^{o}\}$ of multitemporal descriptors that models the multitemporal behaviors of the scene. For example, $D_j^k = \Delta_j^k(D_{1,j}^k, D_{2,j}^k)$, $k = \{px, p, o\}$, $j = 1, \ldots, J^k$.

Each single-date descriptor can be a remotely sensed image (acquired by either active or passive sensors), a feature extracted from a remote sensing image, a high level semantic map (e.g., building maps, classification maps), etc. Higher levels can be seen as a simplification of the original images that reduces the high variability that characterizes the radiometry at pixel level and therefore the dependency on the sensor properties and the acquisition conditions. Generally, at the object level, the descriptor depends only on the object on the ground $D_{i,j}^{o}(\mathrm{Grd}_i)$. From now on, for simplification of the notation, the descriptor dependencies will be left implicit.

Given a problem and the goal of detecting a specific kind of radiometric change, different images (or data) may be available for the acquisition times. Depending on the images and the application problem, an adequate set of descriptors should be extracted and properly combined to allow the detection of the semantic of radiometric changes of interest according to the selected strategy. Based on the available *a priori* information, three approaches to descriptor extraction can be adopted: 1) simplification based; 2) prediction based; and 3) hybrid.

The *simplification-based* approach is bottom–up and assumes that a pair of remote sensing images $D_{1,1}^{px}$ and $D_{2,1}^{px}$ is available. This is the most common situation. Multitemporal images can be acquired by: 1) the same sensor (in this case they present similar characteristics in terms of radiometric properties and geometry if the same view angle is used in the acquisition); 2) by sensors based on similar technology, e.g., two kinds of passive sensors (in such a situation the multitemporal images show a certain level of similarity, but they may differ in terms of radiometric and geometric properties depending on the sensor itself); and 3) by sensors based on different technologies (in this case, images have completely different properties). The simplification approach may be applied with different goals. The first one is to extract proper descriptors from the images that emphasize radiometric changes with a specific semantic meaning, by removing (or mitigating) the components that are not relevant for the specific problem. The second one is to extract descriptors (especially in the case of multisensor data sets) that make it possible the direct comparison between available multitemporal information which would be otherwise unfeasible due to the different characteristics of images acquired by different sensors. This is done by defining descriptors that represent primitives in which the dependence from the sensor and the acquisition conditions are filtered out (e.g., lines, specific objects). Each simplification step leads to the definition of a meta-level (which could be represented either in a raster or a vector form), which contributes to extract the semantic of radiometric changes. Meta-levels can be computed according to strategies that reach different tradeoffs between simplification and fidelity to the radiometric content of the original images. To this end, a simplification function $\Phi_j^k(\cdot)$ is introduced in the notation that depends on the desired output meta-level (pixel, primitive, or object meta-levels) and on the kind of available data. In order to compute the desired descriptor $D_{i,j}^k$, the function

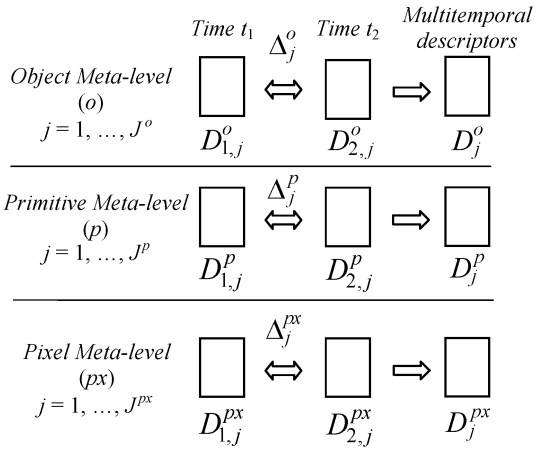

Fig. 8. *Schematic multilevel representation of multitemporal information according to the proposed framework.*

$\Phi_j^k(\cdot)$ is applied to a lower meta-level descriptor (according to the multilevel representation given in Fig. 8). The descriptor $D^k_{1,j}$ can be computed as $\Phi_j^k(D^s_{1,t})$. Fig. 9(a) illustrates the simplification process. In the following, for the sake of simplicity, the dependency of $\Phi_j^k(\cdot)$ from lower level descriptors is omitted.

An alternative conceptual approach to the comparison of images acquired by different sensors (or of an image with a digital map) is to transform one image into the domain of the other according to a proper *prediction-based* approach. This can be done in specific applications, by extracting the objects of interest from one image (or one map) and using the associated meta-level for predicting the effect of the object on the second image. In this way, the comparison can be performed directly in the image domain. The prediction-based approach is top–down and assumes the availability of a high level abstraction descriptor $D^o_{i,j}$ (e.g., a classification map, a cadastral map). From it, lower level descriptors can be predicted (e.g., the spectral signature of buildings, the presence of shadows) by accurately modeling the dependency from the sensor and acquisition conditions. It is worth noting that the prediction process leads only to an estimation of information in lower abstraction meta-levels. This becomes clear if we assume to use the prediction process to derive the lowest abstraction meta-level $D^{px}_{i,j}$, i.e., to predict how the image acquired on the area of interest would have been if acquired with a given remote sensor. Such a predicted image can be similar to a real acquired image, but not identical (depending on the effectiveness of the adopted prediction method). To this end, a prediction function at pixel, primitive, and object meta-levels $\Psi_j^k(\cdot)$ is introduced that depends on the kind of available data and on the desired predicted descriptor. In order to compute the desired descriptor $D^k_{i,j}$, the function $\Psi_j^k(\cdot)$ is applied to a higher (according to the multilevel representation given in Fig. 8) meta-level descriptor. As an example, the descriptor $D^k_{i,j}$ can be computed as $\Psi_j^k(D^s_{i,t})$. Fig. 9(b) exemplifies the prediction process. In the following, for the sake of simplicity, the dependency of $\Psi_j^k(\cdot)$ from higher level descriptors is omitted. Once the desired meta-level has been predicted, proper comparison operators that allow one the extraction of multitemporal information for change detection should be applied.

Simplification and prediction can be jointly used in the context of an *hybrid meta-level* approach to handle complex situations in which available multitemporal descriptors are nonhomogeneous. As an example, for the t_1 image, a descriptor at object $D^o_{1,j}$ level is available (e.g., a cadastral map) whereas a descriptor at pixel level $D^{px}_{2,j}$ is given (e.g., a remotely sensed image) for t_2. In order to perform change detection in such situations, one can use a simplification approach to transform the image information $D^{px}_{2,j}$ into the object descriptor $D^o_{2,j}$, or a prediction approach to transform the object information $D^o_{1,j}$ in an estimate of the pixel information $D^{px}_{1,j}$. As an alternative, the information available in the two descriptors could be projected into a common meta-level of abstraction such that a comparison becomes feasible. This meta-level should represent the same kind of objects (or primitives) for the two acquisitions. Therefore, prediction should be performed from $D^o_{1,j}$ in order to obtain lower meta-levels of information representation, whereas simplification should be applied to $D^{px}_{2,j}$ for computing higher meta-levels [Fig. 9(c)]. The descriptors, obtained with different techniques and algorithms, should be then reported in the same geographical reference system. Whenever this constraint is satisfied, the extraction of descriptors from the original images can be sensor dependent and also very dissimilar from image to image (e.g., building detection in VHR SAR [73] and multispectral images [88]).

Once the meta-levels have been generated by processing multitemporal images separately as in [5] or also by considering the results of a comparison between images at a given meta-level (e.g., analysis of the difference image obtained at a pixel level), they can be jointly involved in the detection of a specific radiometric change according to proper meta-level fusion strategies. This radiometric change may be relevant or nonrelevant to the end user depending on whether the selected approach to change detection is based on direct extraction of relevant changes or on the extraction by cancellation, respectively. To extract relevant or nonrelevant changes, different decision strategies for meta-level fusion can be adopted. Logical combination of single level can be applied, which uses simple rules that implement the rationale adopted in the multitlevel representation of the information. More complex strategies could be used, like the hierarchical binary decision trees or production systems that implement rule-based techniques that can infer logical consequences from the meta-levels [89]. Other possible strategies are based on the use of the meta-levels as input

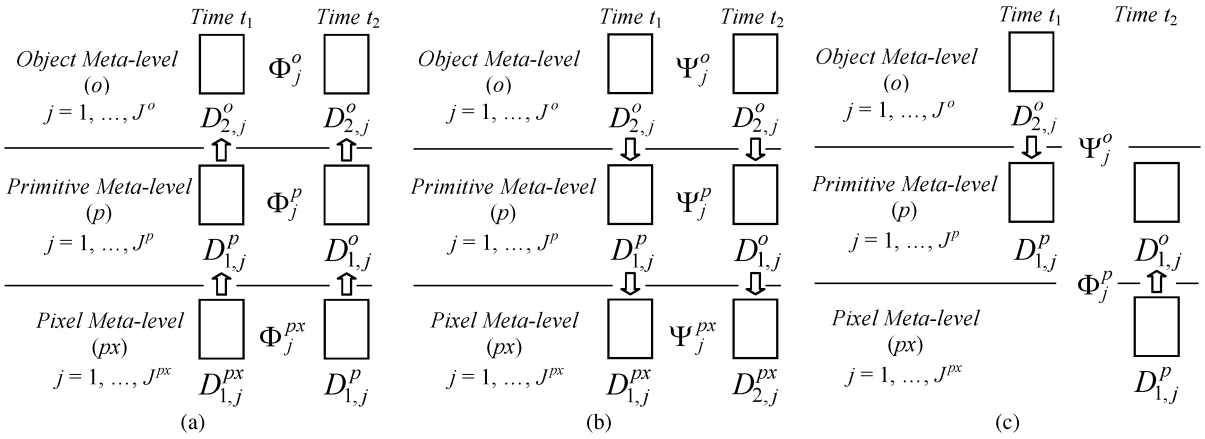

Fig. 9. *Schematic representation of the approaches to the multilevel modeling of multitemporal information: (a) simplification (bottom–up) approach, (b) prediction (top–down) approach, and (c) hybrid approach.*

to an unsupervised clustering algorithm. Of course, the most reliable choice depends on the specific application and on the related multilevel modeling of the problem.

This step can become more or less automatic depending on whether automatic methods exist or can be designed for the specifically addressed problem.

VI. ILLUSTRATIVE EXAMPLE OF APPLICATION OF THE PROPOSED FRAMEWORK

To illustrate how the proposed framework can be employed in the solution of a real problem and to demonstrate its usefulness and effectiveness, a real change-detection problem has been analyzed. In detail, two VHR images acquired by the QuickBird sensor on a portion of the city of Trento, Italy, in July 2005 and October 2006, respectively, were considered. The two images were acquired with different view angles: 1.14° for the July image and 9.8° for the October one. The QuickBird sensor collects panchromatic images at 0.7-m resolution and multispectral images with four spectral channels (blue, 450–520 nm; green, 520–600 nm; red, 630–690 nm; and near-infrared, 760–900 nm) at 2.8-m resolution. In the preprocessing phase, the two images were: 1) pan-sharpened; 2) radiometrically corrected; and 3) coregistered. Pan-sharpened images were computed as we expect that pan-sharpening can improve change detection, as demonstrated in previous work [46]. For this purpose, we applied the Gram–Schmidt procedure implemented in the ENVI software package [90] to the panchromatic channel and the four bands of the multispectral images. The registration process was carried out by using a simple polynomial function of order 2 according to 14 ground control points and by applying a nearest neighbor interpolation. Fig. 10 shows the pan-sharpened multitemporal images of 450 × 400 pixels used in the illustrative example. This small portion of the images was selected because it shows different kinds of radiometric changes and for it *a priori* information on the changes occurred on the ground was available. Concerning radiometric corrections, we simply normalized the images by subtracting from each spectral channel of the two images its mean value [14], [27].

Despite the fact that some simple preprocessing steps have been carried out, as will be clear from Section VI-A, the selected test site shows many of the challenges typical of VHR images (i.e., radiometric changes nonrelevant to the end user).

A. Definition of the Tree of Radiometric Changes

According to the proposed procedure, in the first step, the multitemporal data set has been analyzed according to the taxonomy described in Section IV-A in order to detect the radiometric changes present between the two dates and to define the tree of radiometric changes associated with the considered problem and data. The analyzed images are affected by changes due to acquisition conditions and changes occurred on the ground. With regard to changes occurred on the ground (Ω_{Grd}), we can observe changes in the phenological state of the vegetation (Ω_{Veg}) due to the different acquisition seasons [changes in the apple trees (ω_{at}) in the center of the image, and in the grassland (ω_{gl}) in the right-hand side], and changes due to anthropic activities (Ω_{Ant}) [a new building in the center (ω_b)], i.e., $\Omega_{\mathrm{Veg}} = \{\omega_{at}, \omega_{gl}\}$, $\Omega_{\mathrm{Ant}} = \{\omega_b\}$, and $\Omega_{\mathrm{Grd}} = \{\Omega_{\mathrm{Veg}}, \Omega_{\mathrm{Ant}}\}$. In this specific case, changes due to acquisition conditions are associated with both the different view angles of the sensor and the different sunrays incidence angle (caused by the acquisition seasons). Such factors generate small differences in the appearance of objects (slightly different parts of the same objects are visible in the two acquisitions), leading to geometric distortions and thus to residual misregistration (ω_{rn}) even after alignment of images. Furthermore, we can see differences in shadows which show slightly different

(a) (b)

Fig. 10. *True color composition of the pan-sharpened multispectral QuickBird VHR images: (a) image acquired in October 2005; and (b) image acquired in July 2006. Yellow circles and white arrows highlight change locations.*

directions. They are longer in the October image than in the July one, leading to radiometric changes (ω_{sh}) not related to real changes on the ground. The latter kinds of change belong to the set of differences in the acquisition system (Ω_{Sys}) and represent nonrelevant radiometric changes from the application viewpoint, i.e., $\Omega_{\mathrm{Sys}} = \{\omega_{sh}, \omega_{rn}\}$. In order to reduce the impact of ω_{rn} and ω_{sh} on the detection of changes of interest, their behaviors should be explicitly handled. According to this analysis and to the taxonomy described in Section IV-A, the tree of the radiometric changes for the problem is shown in Fig. 11(a). Since our goal is to detect all the changes occurred on the ground $\Omega_{\mathrm{Grd}} = \{\Omega_{\mathrm{Veg}}, \Omega_{\mathrm{Ant}}\}$ by removing the effects of ω_{rn} and ω_{sh}, in our experiments, all the mentioned changes on the ground are treated as a single class Ω_{Grd}. Thus, the pruned tree that drives the definition of the change-detection architecture is shown in Fig. 11(b).

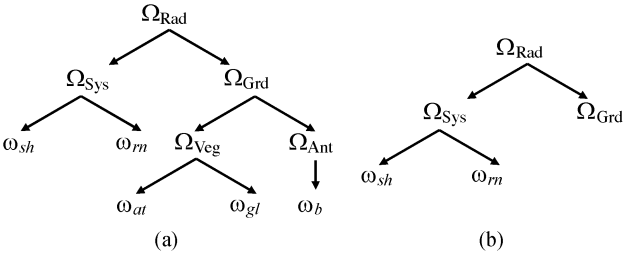

Fig. 11. *Tree of radiometric changes for the considered problem: (a) complete tree describing all radiometric changes; and (b) pruned tree that describes the radiometric changes relevant to the final goal of the specific change-detection problem.*

In the following, the architecture that solves this problem is described pointing out the strategy to combine radiometric changes in order to compute the final change-detection map and the descriptors for modeling them.

B. Strategy for the Detection of Radiometric Changes of Interest

We analyzed the tree of radiometric changes for defining the strategy to use for the detection of the changes of interest. Since we are interested in all the changes occurred on the ground [i.e., changes in the apple trees (ω_{at}), in the grassland (ω_{gl}), and the new building (ω_b)], it is not easy to implement a direct detection of them as they have different properties that are difficult to be directly modeled and extracted as a single class. Thus, we approached the problem according to the differential detection by cancellation of the radiometric changes associated with the sources of noise [i.e., residual misregistration (ω_{rn}) and shadow differences (ω_{sh})]. Accordingly, we first extracted all the radiometric changes from the images, then we detected the radiometric changes associated with the registration noise and with differences in shadows. Finally, we applied a differential analysis according to a proper cancellation algorithm [see Fig. 7(a)]. Thus, first radiometric changes (Ω_{Rad}) have been separated from radiometrically unchanged pixels $\overline{\Omega}_{\mathrm{Rad}}$ ($\overline{\Omega}_{\mathrm{Rad}}$ is the set complementary to Ω_{Rad}). Radiometrically changed pixels are further analyzed to identify and isolate changes associated with differences in the *system acquisition conditions* (Ω_{Sys}), i.e., shadows (ω_{sh}) and registration noise (ω_{rn}). Once noise sources have been identified they are removed from the map of radiometric changes according to a context-based implementation of the fusion strategy. This map is still

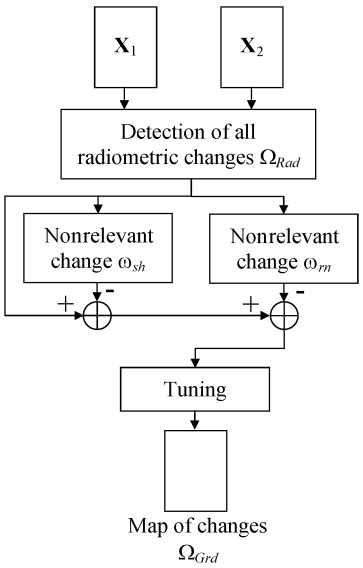

Fig. 12. *Block scheme of the general architecture applied to the solution of the considered change-detection problem.*

affected by residual errors induced by noisy components. Thus, a step of tuning is performed on the basis of the properties of unchanged pixels and radiometrically changed pixels relevant to the user to generate a refined changed-detection map. The general architecture is given in Fig. 12.

C. Multiscale Representation of the Multitemporal Information

In order to extract radiometric changes and to identify changes associated with shadows and registration noise, different techniques have been adopted, which are based on the use of a proper set of multilevel descriptors of the multitemporal information (see Section V-B). To this end, single date and multitemporal descriptors have been computed for extracting different semantics from the images. These descriptors are as follows.

Single Date Descriptors: 1) *pixel level descriptor 1*: vectors of the spectral channels of the images at the two acquisition dates $D^{px}_{1,1}$, $D^{px}_{2,1}$; and 2) *pixel level descriptor 2*: shadow indexes $D^{px}_{1,2}$, $D^{px}_{2,2}$ extracted from $D^{px}_{1,1}$, $D^{px}_{2,1}$, respectively, i.e., $D^{px}_{1,2} = \Phi^{px}_1(D^{px}_{1,1})$ and $D^{px}_{2,2} = \Phi^{px}_1(D^{px}_{2,1})$, where $\Phi^{px}_1(.)$ is defined according to [86]. First, images $D^{px}_{i,1}$ are transformed into the HSI representation. In this feature space, the shadow index is defined as

$$D^{px}_{i,2} = \frac{H_i + 1}{I_i + 1} \tag{3}$$

where H_i and I_i are the hue and intensity values of image $D^{px}_{i,1}$ $(i = \{1, 2\})$.

Multitemporal Descriptors: 1) *pixel level descriptor 1*: magnitude of the multispectral change vector D^{px}_1 obtained by pixel-by-pixel spectral vector difference of $D^{px}_{1,1}$, $D^{px}_{2,1}$, i.e., $D^{px}_1 = \Delta^{px}_1(D^{px}_{1,1}, D^{px}_{2,1})$, where $\Delta^{px}_1(.)$ computes the difference between vectors and applies the magnitude operator [31], i.e.,

$$D^{px}_1 = \sqrt{\left(D^{px}_{1,1} - D^{px}_{2,1}\right)^2}; \tag{4}$$

2) *pixel level descriptor 2*: shadow change index D^{px}_2 obtained by the subtraction of $D^{px}_{1,2}$, $D^{px}_{2,2}$, $D^{px}_2 = \Delta^{px}_2(D^{px}_{1,2}, D^{px}_{2,2})$, i.e.,

$$D^{px}_2 = D^{px}_{1,2} - D^{px}_{2,2}; \tag{5}$$

3) *primitive level descriptor 1*: probability of residual registration noise D^p_1 obtained according to the approach proposed in [14] where $D^{px}_{1,1}$ and $D^{px}_{2,1}$ are properly analyzed and the information on the probability to have registration noise is extracted, i.e., $D^p_1 = \Delta^P_1(D^{px}_{1,1}, D^{px}_{2,1})$ (see [14] for more details).

As the specific objective of the experiments is to detect regions affected by changes occurred on the ground, we are not interested in identifying the specific label associated to the target changed objects; thus, the object level is not considered in this example and the simplification process is limited to the pixel and the primitive ones.

D. Detailed Block Scheme

According to the tree of radiometric changes and to the detection by cancellation architecture, the aforementioned primitives have been combined in order to obtain the map of all radiometric changes and the ones associated with nonrelevant changes due to: 1) shadows; and 2) registration noise. The map of radiometric changes is obtained by modeling the statistical distribution of magnitude of multispectral difference vectors D^{px}_1 as a sum of two distributions associated with the class of changed and no-changed pixels, respectively. Class conditional densities are modeled as being Gaussian and thus fully described by their mean value and variance. To separate the two classes, the Bayesian decision rule for minimum error is applied according to [31]. Statistical class parameters have been estimated with the unsupervised method presented in [31] based on the expectation–maximization algorithm [31], [69], [91]–[93]. This operation leads to the generation of a binary map that separates radiometrically changed pixels (Ω_{Rad}) from the unchanged ones $(\overline{\Omega}_{\mathrm{Rad}})$. Concerning shadows, the information of the D^{px}_2 descriptor is used. In order to detect shadow changes, pixels already detected as

unchanged are removed from the analysis. Remaining pixels, similarly to what was done with D_1^{px}, are modeled as a sum of two statistical distributions associated with shadow (ω_{sh}) and no-shadow ($\overline{\omega}_{sh}$) classes. Class conditional densities are modeled as being Gaussian and thus fully described by their mean value and variance. Similarly as before, the statistical class parameters are estimated according to the unsupervised method presented in [31] and [69] and using the expectation–maximization algorithm, and shadow and no-shadow classes are separated by applying the Bayesian decision rule for minimum error. The method in [14] is applied for extracting the radiometric changes associated with registration noise. First, the distribution of the registration noise is obtained in the polar change vector analysis domain according to a multiscale analysis [42]. Then, it is thresholded for generating the map of radiometric changes associated with registration noise. Finally, the fusion step is performed according to a context-based strategy where the spatial context information is modeled by a system of adaptive multitemporal neighborhoods. The neighborhood system is obtained by a two-step procedure. In the first step, each multitemporal image is segmented independently [94]. The multitemporal fusion of these maps leads to the definition of regions that have the property to be homogeneous both in space and time: the multitemporal parcels. In order to assign a homogeneous label to each identified parcel the labels assumed by the pixels in it are analyzed. If the sum of pixels with a label equal to $\overline{\Omega}_{\mathrm{Rad}}$, ω_{sh}, and ω_{rn} corresponds to the majority of pixels, then the parcel is assigned to the class of no-changed pixels $\Omega_{nc} = \{\overline{\Omega}_{\mathrm{Rad}}, \Omega_{\mathrm{Sys}}\}$, where $\Omega_{\mathrm{Sys}} = \{\omega_{sh}, \omega_{rn}\}$. Otherwise the parcel is thought as being candidate to be associated with the class of changes occurred on the ground (Ω_{Grd}) as it contains a majority of radiometrically changed pixels relevant to the end user (i.e., not associated to registration noise or shadow). Of course more complex strategies could be used in the fusion step.

In order to take a final decision on these candidate parcels, the whole procedure can be applied again to them in order to better tune the decision threshold on the parcels candidate to be changed. This tuning step allows one to reduce missed/false alarms caused by the noise present when all radiometric changes are analyzed together (i.e., when the contributions of radiometric changes associated with ω_{sh} and ω_{rn} are considered). In this way, the decision step can be better tuned on the properties of the radiometric changes of interest. At the end of the whole process (first and second iterations) parcels reclassified as Ω_{Sys} and $\overline{\Omega}_{\mathrm{Rad}}$ are associated with the class of no-changed pixels $\Omega_{nc} = \{\overline{\Omega}_{\mathrm{Rad}}, \Omega_{\mathrm{Sys}}\}$. All the others are classified as changes of interest Ω_{Grd}. Fig. 13 shows the block scheme of the resulting change detection system. In this case, the designed procedure led to a fully automatic system (only few parameters need to be set manually in the phase of system optimization). However, more in general, depending on the problem and on the algorithms, the designed system might be either automatic or semiautomatic. Note that even if the scheme is complex, it has been obtained according to a relatively simple top–down approach driven by the proposed framework.

E. Experimental Results

This section presents the results obtained by the system designed on the basis of the proposed framework for

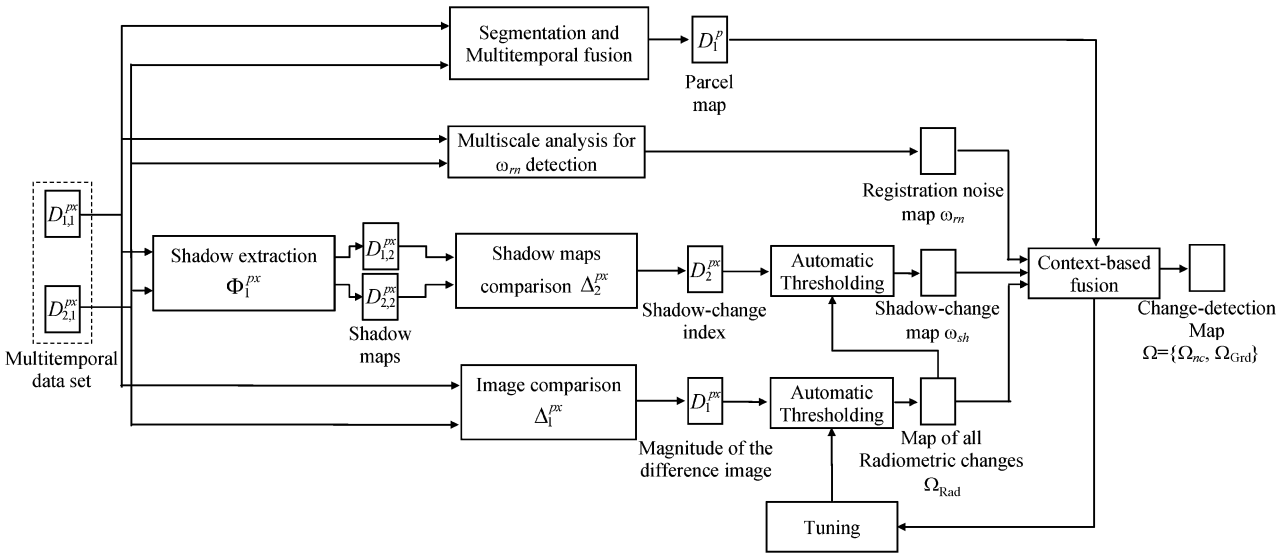

Fig. 13. *Detailed block scheme of the change-detection system defined by using the proposed framework for solving the change-detection problem considered in the example.*

solving the specific change-detection problem. Such results are compared with those achieved by: 1) pixel-based change vector analysis [31]; and 2) parcel-based change vector analysis [30], which uses multitemporal parcels for modeling the spatial context information.

In order to perform a quantitative comparison, a reference map has been defined by photointerpretation and according to the authors' *a priori* knowledge on the scene. The map shows 149 319 unchanged pixels (white color) and 14 081 changed pixels (black color) [Fig. 14(c)]. Changed pixels include all radiometric changes relevant to the application (refer to the beginning of Section IV-A for their description). The map has been used for a relative ranking of methods in the experimental analysis.

As expected, the proposed system achieves the highest overall accuracy, gaining about 3% with respect to the pixel-based change vector analysis (CVA). Moreover, it performs also better than the parcel-based change vector analysis (increase of accuracy about 2%). This latter observation highlights the fact that adaptive context-based change-detection methods based only on the radiometry of multispectral changes without an explicit modeling of different causes of radiometric change are not enough to obtain effective change-detection results. In greater detail, the performance of pixel- and parcel-based CVA is significantly affected by a high amount of false alarms. These are mainly due to the effects of residual registration noise and changes in shadow regions that are true

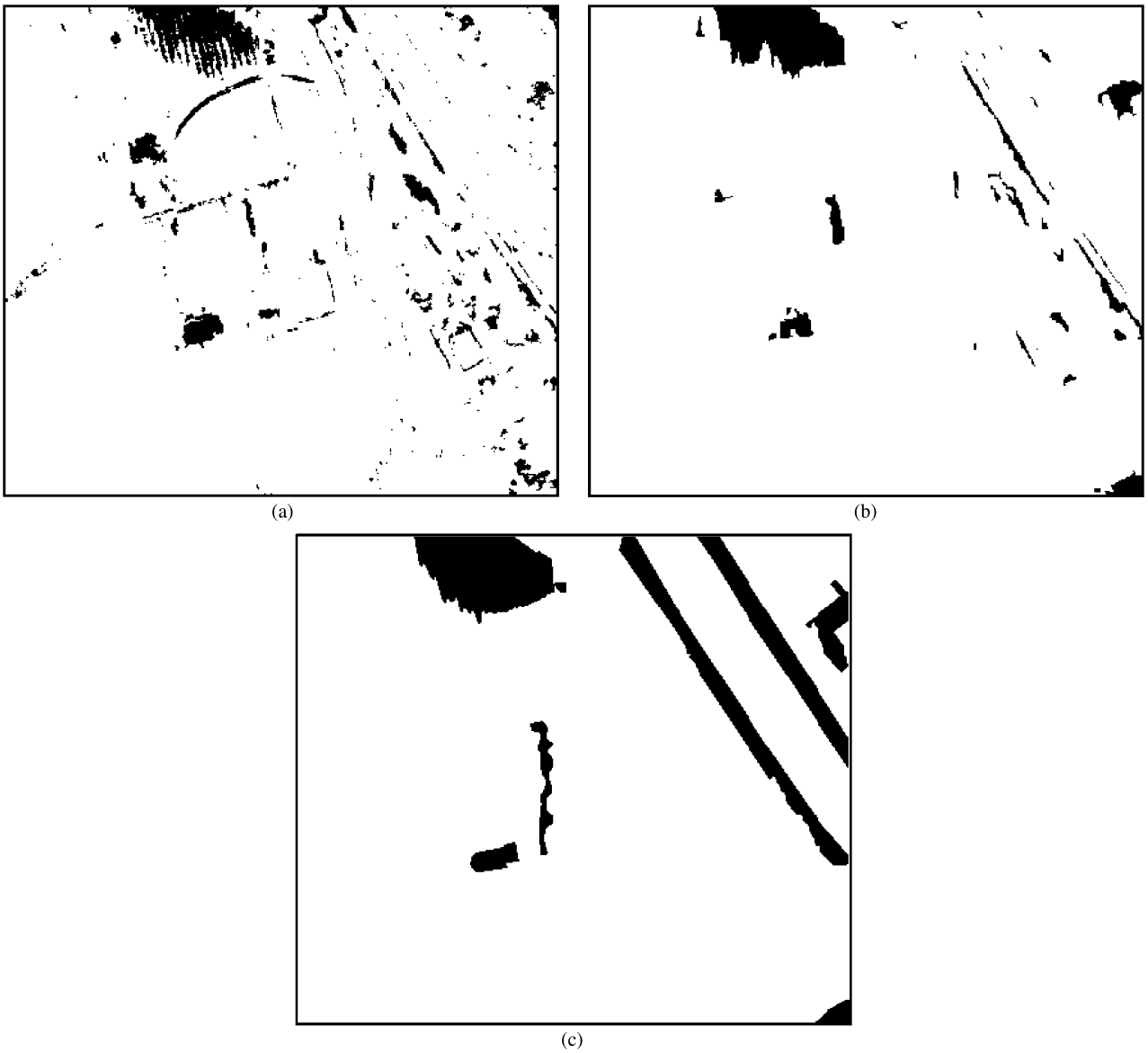

Fig. 14. ***Change-detection maps obtained by (a) the pixel-based change vector analysis, and (b) the proposed method. Reference map of changes of interest (black color).***

Table 1 False Alarms, Missed Alarms, Overall Errors, and Overall Accuracy Provided by the Considered Methods

Change-detection approach	False alarms	Missed alarms	Overall error	Overall accuracy (%)
CVA (pixel-based)	5005	9924	14929	90.86
CVA (parcel-based)	3537	10261	13798	91.56
Proposed System	1470	8480	9950	93.91

radiometric changes, which however are not of interest to the end user. Thanks to the explicit modeling of the sources of radiometric change, such kinds of changes do not appear in the change-detection map obtained with the method developed on the basis of the proposed framework, which results in almost half the false alarms with respect to the parcel-based CVA (1470 versus 3537) and one third with respect to pixel-based CVA (1470 versus 5005) (see Table 1). Moreover, the proposed method results in a lower amount of missed changes of interest. Such errors are mainly due to an overestimation of the decision threshold value caused by the population of radiometric changes associated with registration noise and shadows present in the difference image. The tuning mechanism introduced in the presented system after the cancellation of nonrelevant radiometric changes reduces the impact of this kind of errors, which decreases by around 1600 pixels. The qualitative analysis of the change-detection maps in Fig. 14 confirms the quantitative results. A detailed analysis of the obtained maps and of the amount of missed alarms points out that some of the changes occurred on the ground are not accurately detected also from the proposed technique. This is mainly due to the fact that these changes are not sufficiently visible in the images and thus cannot be detected irrespectively of the adopted change-detection method.

This example points out how the proposed framework can drive the definition of a change-detection system that can better model the complexity of VHR multispectral images.

VII. DISCUSSION AND CONCLUSION

In this paper, a general framework for designing effective change-detection architectures for multitemporal VHR images has been introduced. The framework is based on the observation that the complexity of VHR images results in many possible sources of radiometric changes among images acquired on the same geographical area at different times. These radiometric changes are often not related to changes occurred on the ground or may be associated with changes not relevant to the specific application. Despite the fact that this effect was observed also in moderate/high-resolution images, as explained in the paper, the phenomenon becomes very critical in VHR satellite images, where the geometrical details strongly emphasize the possibility to identify radiometric changes which are not related to changes on the ground. Thus, it becomes mandatory to modify the perspective of unsupervised change-detection techniques, from the capability to detect radiometric changes (both with pixel-based or context-sensitive techniques), to the capability of detecting changes with a semantic meaning of interest for end users. To this end, an effort is necessary to model and extract the semantic meaning of each source of radiometric change in order to isolate changes of interest, which is commonly not the case in most of the state-of-the-art techniques.

For addressing the problem, we first defined a complete taxonomy of radiometric changes that may occur in VHR images, by distinguishing between sources of noise and kinds of change occurred on the ground (and analyzing their causes). Based on this taxonomy, a general approach to the design of a change-detection architecture was defined, which is based on the idea of identifying, modeling, extracting, and taking advantage of the semantic meaning of radiometric changes. The approach starts from the definition of the tree of radiometric changes that models the structure of the expected radiometric changes in the change-detection problem and drives the next steps of the system design. According to the tree of radiometric changes it is possible to define architectures for change detection by means of two strategies: 1) direct identification of changes relevant to the end user; or 2) indirect identification of changes relevant to the end user by cancellation of nonrelevant changes. Once the strategy has been selected, a multilevel description of multitemporal information is defined, including pixel-based measurements, geometric and statistical primitives as well as object-based representations. A set of algorithms is then defined in order to properly combine the multilevel information, extract specific radiometric changes, and associate them with their semantic meaning within the selected strategy.

Another important concept discussed in this work is related to how the multilevel representation of multitemporal information in VHR images can be obtained, i.e., by simplification or prediction. The two options, which are often used in the image processing domain, are seen as alternative tools (which can also be used jointly) that can

be used for a homogeneous and improved representation of the information that should be modeled in the change-detection process on VHR data. They are also effective methodologies for potentially addressing multisource and multisensor change-detection problems.

In this paper, we have also presented an illustrative example in which the proposed general framework is employed for defining an unsupervised change-detection system and the related algorithms for a specific application context. Starting from the taxonomy of radiometric changes, we have first identified the tree of radiometric changes that describes the problem. Then, we have defined a change-detection scheme based on the differential detection of radiometric changes of interest by cancellation. In this context, all the relevant sources of noninteresting radiometric changes (in our case, the registration noise and the differences in shadows) have been modeled for extracting their semantic meaning and isolating changes of interest in the final change-detection map. This was done considering a context-sensitive decision approach based on the use of multitemporal parcels. Experimental results point out that an effective modeling of sources of radiometric changes can result in a significant improvement of the change-detection accuracy with respect to standard unsupervised change-detection methods. Moreover, the proposed procedure for the definition of the change-detection system results in a top–down systematic and conceptually simple approach to the design of complex change-detection architectures that may integrate many components and algorithms. The presented example should be seen as an illustration of how the change-detection problem should be addressed considering the proposed framework. Of course different implementations of the different stages of the change-detection architecture can be considered according to the specific problem, to the images, and to the end user's needs.

As a final remark, we would like to emphasize that the proposed framework defines important guidelines for the development of a new generation of change-detection methods that can properly analyze multitemporal VHR remote sensing images taking into account the intrinsic complexity associated with these data. Nevertheless, the framework can be easily adapted and applied to other applicative domains. The change-detection system designed according to the proposed framework can be either automatic or semiautomatic. The level of automation depends on the specific techniques and algorithms that are used as components of the general change-detection architecture.

As future developments of this work, we are now investigating strategies that, starting from the general approach presented in this paper, can be used for addressing specific change-detection problems with VHR images (both multispectral and SAR). ■

Table 2 Mathematical Notation

Symbol	Description
Ω_{Rad}	Set of radiometric changes
Ω_{Acq}	Set of changes due to acquisition conditions
Ω_{Grd}	Set of changes occurred on the ground
Ω_{Atm}	Set of changes due to atmospheric conditions
Ω_{Sys}	Set of changes due to the acquisition system
Ω_{Veg}	Set of changes due to the phenological state of the vegetation
Ω_{Env}	Set of changes due to the environmental conditions
Ω_{Dis}	Set of changes due to the effects of natural disasters
Ω_{Ant}	Set of changes due to the anthropic activity
i	Acquisition time index
$\boldsymbol{D}_i$	Set of descriptors of the image acquired at time i
$D_{i,j}^k$	jth descriptor of meta-level k at time i
k	Meta-level identifier $k=\{px,p,o\}$
j	Descriptor identifier $j = 1,\ldots,J^k$
J^k	Highest descriptor index at meta-level k
$\Delta_j^k(\cdot)$	Function for extracting the jth multitemporal descriptor at meta-level k
$\boldsymbol{D}$	Set of multitemporal descriptors
D_j^k	jth multitemporal descriptor of meta-level k
$\Phi_j^k(\cdot)$	jth simplification function of meta-level k
$\Psi_j^k(\cdot)$	jth prediction function of meta-level k
ω_{at}	Class of vegetation changes related to apple trees ($\omega_{at} \in \Omega_{Veg}$)
ω_{gl}	Class of vegetation changes related to the grassland ($\omega_{gl} \in \Omega_{Veg}$)
ω_b	Class of anthropic changes related to buildings ($\omega_b \in \Omega_{Ant}$)
ω_{rn}	Class of changes due to registration noise ($\omega_{rn} \in \Omega_{Sys}$)
ω_{sh}	Class of changes due to shadow ($\omega_{sh} \in \Omega_{Sys}$)

APPENDIX

The mathematical notation used in the paper is listed in Table 2. Symbols are listed in the appearance order.

Acknowledgment

The authors would like to thank S. Demetri for the contribution given in the experimental part of this work.

REFERENCES

[1] A. J. Radke, S. Andra, O. Al-Kofahi, and B. Roysam, "Image change detection algorithms: A systematic survey," *IEEE Trans. Image Process.*, vol. 14, no. 3, pp. 294–307, Mar. 2005.

[2] P. R. Coppin, I. Jonckheere, and K. Nachaerts, "Digital change detection in ecosystem monitoring: A review," *Int. J. Remote Sens.*, vol. 25, no. 9, pp. 1565–1596, May 2004.

[3] D. Lu, P. Mausel, E. Brondízio, and E. Moran, "Change detection techniques," *Int. J. Remote Sens.*, vol. 25, no. 12, pp. 2365–2407, Jun. 2004.

[4] A. Singh, "Digital change detection techniques using remotely-sensed data," *Int. J. Remote Sens.*, vol. 10, no. 6, pp. 989–1003, 1989.

[5] F. Bovolo, "A multilevel parcel-based approach to change detection in very high resolution multitemporal images," *IEEE Geosci. Remote Sens. Lett.*, vol. 6, no. 1, pp. 33–37, Jan. 2009.

[6] R. A. Rensink, "Change detection," *Annu. Rev. Psychol.*, vol. 53, pp. 245–277, 2002.

[7] S. Spotorno and S. Faure, "Change detection in complex scenes: Hemispheric contribution and the role of perceptual and semantic factors," *Perception*, vol. 40, pp. 5–22, 2011.

[8] S.-S. Ho and H. Wechsler, "A martingale framework for detecting changes in data streams by testing exchangeability," *IEEE Trans. Pattern Anal. Mach. Intell.*, vol. 32 no. 12, pp. 2113–2127, Dec. 2010.

[9] C. Galindo, A. Saffiotti, S. Coradeschi, P. Buschka, J. A. Fernández-Madrigal, and J. González, "Multi-hierarchical semantic maps for mobile robotics," in *Proc. IEEE/RSJ Int. Conf. Intell. Robots Syst.*, 2005, pp. 2278–2283.

[10] C. Xu, J. Cheng, Y. Zhang, Y. Zhang, and H. Lu, "Sports video analysis: Semantics extraction, editorial content creation and adaptation," *J. Multimedia*, vol. 4, no. 2, pp. 69–79, 2009.

[11] C.-Y. Fang, S.-W. Chen, and C.-S. Fuh, "Automatic change detection of driving environments in a vision-based driver assistance system," *IEEE Trans. Neural Netw.*, vol. 14, no. 3, pp. 646–657, May 2003.

[12] O. Al-Kofahi, R. J. Radke, B. Roysam, and G. Banker, "Automated semantic analysis of changes in image sequences of neurons in culture," *IEEE Trans. Biomed. Eng.*, vol. 53, no. 6, pp. 1109–1123, Jun. 2006.

[13] R. Pique-Regi, A. Ortega, A. Tewfik, and S. Asgharzadeh, "Detecting changes in the DNA copy number," *IEEE Signal Process. Mag.*, vol. 29, no. 1, pp. 98–107, Jan. 2012.

[14] S. Marchesi, F. Bovolo, and L. Bruzzone, "A context-sensitive technique robust to registration noise for change detection in VHR multispectral images," *IEEE Trans. Image Process.*, vol. 19, no. 7, pp. 1877–1889, Jul. 2010.

[15] P. Lu, A. Stumpf, N. Kerle, and N. Casagli, "Object-oriented change detection for landslide rapid mapping," *IEEE Geosci. Remote Sens. Lett.*, vol. 8, no. 4, pp. 701–705, Jul. 2011.

[16] M. Molinier, J. Laaksonen, and T. Häme, "Detecting man-made structures and changes in satellite imagery with a content-based information retrieval system built on self-organizing maps," *IEEE Trans. Geosci. Remote Sens.*, vol. 45, no. 4, pp. 861–864, Apr. 2007.

[17] M. Chini, F. Pacifici, W. J. Emery, N. Pierdicca, and F. Del Frate, "Comparing statistical and neural network methods applied to very high resolution satellite images showing changes in man-made structures at rocky flats," *IEEE Trans. Geosci. Remote Sens.*, vol. 46, no. 6, pp. 1812–1821, Jun. 2008.

[18] E. Pagot and M. Pesaresi, "Systematic study of the urban postconflict change classification performance using spectral and applied to very high resolution satellite images showing changes in man-made structures at rocky flats," *IEEE Trans. Geosci. Remote Sens.*, vol. 1, no. 2, pp. 120–128, Feb. 2008.

[19] F. Pacifici and F. Del Frate, "Automatic change detection in very high resolution images with pulse-coupled neural networks," *IEEE Geosci. Remote Sens. Lett.*, vol. 7, no. 1, pp. 58–62, Jan. 2010.

[20] C. Huo, Z. Zhou, H. Lu, C. Chen, and K. Pan, "Fast object-level change detection for VHR images," *IEEE Geosci. Remote Sens. Lett.*, vol. 7, no. 1, pp. 118–122, Jan. 2010.

[21] P. Soille and M. Pesaresi, "Advances in mathematical morphology applied to geosciences and remote sensing," *IEEE Trans. Geosci. Remote Sens.*, vol. 40, no. 9, pp. 2042–2055, Sep. 2002.

[22] M. Volpi, D. Tuia, F. Bovolo, M. Kanevski, and L. Bruzzone, "Supervised change detection in VHR images using contextual information and support vector machines," *Int. J. Appl. Earth Observat. Geoinf.*, to be published.

[23] L. Bruzzone and S. B. Serpico, "An iterative technique for the detection of land-cover transitions in multitemporal remote-sensing images," *IEEE Trans. Geosci. Remote Sens.*, vol. 35, no. 4, pp. 858–867, Jul. 1997.

[24] L. Bruzzone, R. Cossu, and G. Vernazza, "Detection of land-cover transitions by combining multidate classifiers," *Pattern Recognit. Lett.*, vol. 25, no. 13, pp. 1491–1500, 2004.

[25] L. Bruzzone and R. Cossu, "A multiple cascade-classifier system for a robust a partially unsupervised updating of land-cover maps," *IEEE Trans. Geosci. Remote Sens.*, vol. 40, no. 9, pp. 1984–1996, Sep. 2002.

[26] B. Demir, F. Bovolo, and L. Bruzzone, "Detection of land-cover transitions in multitemporal remote sensing images with active-learning-based compound classification," *IEEE Trans. Geosci. Remote Sens.*, vol. 50, no. 5, pt. 2, pp. 1930–1941, May 2012.

[27] F. Bovolo and L. Bruzzone, "A theoretical framework for unsupervised change detection based on change vector analysis in polar domain," *IEEE Trans. Geosci. Remote Sens.*, vol. 45, no. 1, pp. 218–236, Jan. 2007.

[28] F. Bovolo, G. Camps-Valls, and L. Bruzzone, "A support vector domain method for change detection in multitemporal images," *Pattern Recognit. Lett.*, vol. 31, no. 10, pp. 1148–1154, 2010.

[29] L. Bruzzone and D. Fernandez Prieto, "A minimum-cost thresholding technique for unsupervised change detection," *Int. J. Remote Sens.*, vol. 21, no. 18, pp. 3539–3544, 2000.

[30] L. Bruzzone and D. Fernandez Prieto, "An adaptive parcel-based technique for unsupervised change detection," *Int. J. Remote Sens.*, vol. 21, no. 4, pp. 817–822, 2000.

[31] L. Bruzzone and D. Fernández-Prieto, "Automatic analysis of the difference image for unsupervised change detection," *IEEE Trans. Geosci. Remote Sens.*, vol. 38, no. 3, pp. 1170–1182, May 2000.

[32] M. Dalla Mura, J. A. Benediktsson, F. Bovolo, and L. Bruzzone, "An unsupervised technique based on morphological filters for change detection in very high resolution images," *IEEE Geosci. Remote Sens. Lett.*, vol. 5, no. 3, pp. 433–437, Jul. 2008.

[33] T. Celik, "Method for unsupervised change detection in satellite images," *Electron. Lett.*, vol. 46, no. 9, pp. 624–626, Apr. 2010.

[34] T. Celik, "Unsupervised change detection in satellite images using principal component analysis and k-means clustering," *IEEE Geosci. Remote Sens. Lett.*, vol. 6, no. 4, pp. 772–776, Oct. 2009.

[35] G. Moser, E. Angiati, and S. B. Serpico, "Multiscale unsupervised change detection on optical images by Markov random fields and wavelets," *IEEE Geosci. Remote Sens. Lett.*, vol. 8, no. 4, pp. 725–729, Jul. 2011.

[36] A. A. Nielsen, K. Conradsen, and J. J. Simpson, "Multivariate Alteration Detection (MAD) and MAF postprocessing in multispectral, bitemporal image data: New approaches to change detection studies," *Remote Sens. Environ.*, vol. 64, no. 1, pp. 1–19, Apr. 1998.

[37] A. A. Nielsen, "Multiset canonical correlations analysis and multispectral, truly multitemporal remote sensing data," *IEEE Trans. Image Process.*, vol. 11, no. 3, pp. 293–305, Mar. 2002.

[38] L. Bruzzone and D. Fernandez Prieto, "Unsupervised retraining of a maximum-likelihood classifier for the analysis of multitemporal remote-sensing images," *IEEE Trans. Geosci. Remote Sens.*, vol. 39 no. 2, pp. 456–460, Feb. 2001.

[39] T. Celik and K. K. Ma, "Unsupervised change detection for satellite images using dual-tree complex wavelet transform," *IEEE Trans. Geosci. Remote Sens.*, vol. 48, no. 3, pp. 1199–1210, Mar. 2010.

[40] F. Bovolo, S. Marchesi, and L. Bruzzone, "A framework for automatic and unsupervised detection of multiple changes in multitemporal images," *IEEE Trans. Geosci. Remote Sens.*, vol. 50, no. 6, pp. 2196–2212, Jun. 2012.

[41] X. Dai and S. Khorram, "The effects of image misregistration on the accuracy of remotely sensed change detection," *IEEE Trans. Geosci. Remote Sens.*, vol. 36, no. 5, pp. 1566–1577, Sep. 1998.

[42] F. Bovolo, L. Bruzzone, and S. Marchesi, "Analysis and adaptive estimation of the registration noise distribution in multitemporal VHR images," *IEEE Trans. Geosci. Remote Sens.*, vol. 47, no. 8, pp. 2658–2671, Aug. 2009.

[43] D. P. Roy, "The impact of misregistration upon composited wide field of view satellite data and implications for change detection," *IEEE Trans. Geosci. Remote Sens.*, vol. 38 no. 4, pp. 2017–2032, Jul. 2000.

[44] M. Ding, Z. Tian, Z. Jin, M. Xu, and C. Cao, "Registration using robust kernel principal component for object-based change detection," *IEEE Geosci. Remote Sens. Lett.*, vol. 7, no. 4, pp. 761–765, Oct. 2010.

[45] M. Aldrighi and F. Dell'Acqua, "Mode-based method for matching of pre- and postevent remotely sensed images," *IEEE Geosci. Remote Sens. Lett.*, vol. 6, no. 2, pp. 317–321, Apr. 2009.

[46] F. Bovolo, L. Bruzzone, L. Capobianco, A. Garzelli, S. Marchesi, and F. Nencini, "Analysis of the effects of pansharpening in change detection on VHR images," *IEEE Geosci. Remote Sens. Lett.*, vol. 7, no. 1, pp. 53–57, Jan. 2010.

[47] M. L. F. Velloso, F. J. de Souza, and M. Simoes, "Improved radiometric normalization for land cover change detection: An automated relative correction with artificial neural network," in *Proc. IEEE Int. Geosci. Remote Sens. Symp.*, 2002, pp. 3435–3437.

[48] X. Yang and C. P. Lo, "Relative radiometric normalization performance for change detection from multi-date satellite images," *Photogramm. Eng. Remote Sens.*, vol. 66, pp. 967–980, Aug. 2000.

[49] S. Inamdar, F. Bovolo, L. Bruzzone, and S. Chaudhuri, "Multidimensional probability density function matching for pre-processing of multitemporal remote sensing images," *IEEE Trans. Geosci. Remote Sens.*, vol. 46 no. 4, pp. 1243–1252, Apr. 2008.

[50] J. Chen, X. Chen, X. Cui, and J. Chen, "Change vector analysis in posterior probability space: A new method for land cover change detection," *IEEE Geosci. Remote Sens. Lett.*, vol. 8, no. 2, pp. 317–321, Mar. 2011.

[51] W. Luo and H. Li, "Soft-change detection in optical satellite images," *IEEE Geosci. Remote Sens. Lett.*, vol. 8, no. 5, pp. 879–883, Sep. 2011.

[52] L. M. Yang, G. Xian, J. M. Klaver, and B. Deal, "Urban land-cover change detection through sub-pixel imperviousness mapping using remotely sensed data," *Photogramm. Eng. Remote Sens.*, vol. 69, no. 9, pp. 1003–1010, Sep. 2003.

[53] V. Haertel, Y. E. Shimabukuro, and R. Almeida, "Fraction images in multitemporal change detection," *Int. J. Remote Sens.*, vol. 25, no. 23, pp. 5473–5489, Dec. 2004.

[54] D. S. Lu, M. Batistella, and E. Moran, "Multitemporal spectral mixture analysis for Amazonian land-cover change detection," *Can. J. Remote Sens.*, vol. 30, no. 1, pp. 87–100, Feb. 2004.

[55] L. O. Anderson, Y. E. Shimabukuro, and E. Arai, "Multitemporal fraction images derived from Terra MODIS data for analysing land cover change over the Amazon region," *Int. J. Remote Sens.*, vol. 26, no. 11, pp. 2251–2257, 2005.

[56] F. Ling, W. Li, Y. Du, and X. Li, "Land cover change mapping at the subpixel scale with different spatial-resolution remotely sensed imagery," *IEEE Geosci. Remote Sens. Lett.*, vol. 8, no. 1, pp. 182–186, Jan. 2011.

[57] A. Robin, L. Moisan, and S. Le Hégarat-Mascle, "An a-contrario approach for subpixel change detection in satellite imagery," *IEEE Trans. Pattern Anal. Mach. Intell.*, vol. 32, no. 11, pp. 1977–1993, Nov. 2010.

[58] J. P. Kerekes and J. E. Baum, "Spectral imaging system analytical model for subpixel object detection," *IEEE Trans. Geosci. Remote Sens.*, vol. 40, no. 5, pp. 1088–1101, May 2002.

[59] C.-I. Chang and C. M. Brumbley, "A Kalman filtering approach to multispectral image classification and detection of changes in signature abundance," *IEEE Trans. Geosci. Remote Sens.*, vol. 37, no. 1, pp. 257–268, Jan. 1999.

[60] S. Marchesi and L. Bruzzone, "ICA and kernel ICA for change detection in multispectral remote sensing images," in *Proc. IEEE Int. Geosci. Remote Sens. Symp.*, 2009, pp. II-980–II-983.

[61] P. R. Marpu, P. Gamba, and M. J. Canty, "Improving change detection results of IR-MAD by eliminating strong changes," *IEEE Geosci. Remote Sens. Lett.*, vol. 8, no. 4, pp. 799–803, Jul. 2011.

[62] A. A. Nielsen, "The regularized iteratively reweighted MAD method for change detection in multi- and hyperspectral data," *IEEE Trans. Image Process.*, vol. 16, no. 2, pp. 463–478, Feb. 2007.

[63] L. Gueguen, P. Soille, and M. Pesaresi, "Change detection based on information measure," *IEEE Trans. Geosci. Remote Sens.*, vol. 49, no. 11, pp. 4503–4515, Nov. 2011.

[64] N. A. Campbell and H. T. Kiiveri, "Canonical variate analysis with spatially-correlated data," *Austral. New Zealand J. Stat.*, vol. 35, no. 3, pp. 333–344, 1993.

[65] P. C. Smits and A. Annoni, "Updating land-cover maps by using texture information from very high-resolution space-borne imagery," *IEEE Trans. Geosci. Remote Sens.*, vol. 37, no. 3, pp. 1244–1254, May 1999.

[66] G. Healey and D. Slater, "Computing illumination-invariant descriptors of spatially filtered color image regions," *IEEE Trans. Image Process.*, vol. 6, no. 7, pp. 1002–1013, Jul. 1997.

[67] L. Li and M. K. H. Leung, "Integrating intensity and texture differences for robust change detection," *IEEE Trans. Image Process.*, vol. 11, no. 2, pp. 105–112, Feb. 2002.

[68] M. Dalla Mura, J. A. Benediktsson, B. Waske, and L. Bruzzone, "Morphological attribute profiles for the analysis of very high resolution images," *IEEE Trans. Geosci. Remote Sens.*, vol. 48, no. 10, pp. 3747–3762, Oct. 2010.

[69] L. Bruzzone and D. Fernandez Prieto, "An adaptive semi-parametric and context-based approach to unsupervised change detection in multitemporal remote sensing images," *IEEE Trans. Image Process.*, vol. 11, no. 4, pp. 452–466, Apr. 2002.

[70] M. J. Carlotto, "A cluster-based approach for detecting man-made objects and changes in imagery," *IEEE Trans. Geosci. Remote Sens.*, vol. 43, no. 2, pp. 374–387, Feb. 2005.

[71] T. Yamamoto, H. Hanaizumi, and S. Chino, "A change detection method for remotely sensed multispectral and multitemporal images using 3-D segmentation," *IEEE Trans. Geosci. Remote Sens.*, vol. 39, no. 5, pp. 976–985, May 2001.

[72] G. G. Hazel, "Object-level change detection in spectral imagery," *IEEE Trans. Geosci. Remote Sens.*, vol. 39, no. 3, pp. 553–561, Mar. 2001.

[73] D. Brunner, G. Lemoine, and L. Bruzzone, "Earthquake damage assessment of buildings using VHR optical and SAR imagery," *IEEE Trans. Geosci. Remote Sens.*, vol. 48, no. 5, pp. 2403–2420, May 2010.

[74] F. Bovolo and L. Bruzzone, "An adaptive multiscale random field technique for unsupervised change detection in VHR multitemporal images," in *Proc. IEEE Int. Geosci. Remote Sens. Symp.*, 2009, pp. IV-777–IV-780.

[75] T. Celik, "Multiscale change detection in multitemporal satellite images," *IEEE Geosci. Remote Sens. Lett.*, vol. 6, no. 4, pp. 820–824, Oct. 2009.

[76] T. Celik and K.-K. Ma, "Multitemporal image change detection using undecimated discrete wavelet transform and active contours," *IEEE Trans. Geosci. Remote Sens.*, vol. 49, no. 2, pp. 706–716, Feb. 2011.

[77] L. Gómez-Chova, G. Camps-Valls, L. Bruzzone, and J. Calpe-Maravilla, "Mean map kernel methods for semisupervised cloud classification," *IEEE Trans. Geosci. Remote Sens.*, vol. 48, no. 1, pp. 207–220, Jan. 2010.

[78] J. A. Torres Arriaza, F. Guindos Rojas, M. Peralta López, and M. Cantón, "An automatic cloud-masking system using backpro neural nets for AVHRR scenes," *IEEE Trans. Geosci. Remote Sens.*, vol. 41, no. 4, pp. 826–831, Apr. 2003.

[79] A. Wiesmann, T. Strozzi, C. Werner, U. Wegmuller, and M. Santoro, "Microwave remote sensing of alpine snow," in *Proc. IEEE Int. Geosci. Remote Sens. Symp.*, Barcelona, Spain, 2007, pp. 1223–1227.

[80] L. Sahar, S. Muthukumar, and S. P. French, "Using aerial imagery and GIS in automated building footprint extraction and shape recognition for earthquake risk assessment of urban inventories," *IEEE Trans. Geosci. Remote Sens.*, vol. 48, no. 6, pp. 3511–3520, Jun. 2010.

[81] S. Voigt, T. Kemper, T. Riedlinger, R. Kiefl, K. Scholte, and H. Mehl, "Satellite image analysis for disaster and crisis-management support," *IEEE Trans. Geosci. Remote Sens.*, vol. 45, no. 6, pp. 1520–1528, Jun. 2007.

[82] J. Verbesselt, P. Jonsson, S. Lhermitte, J. van Aardt, and P. Coppin, "Evaluating satellite and climate data-derived indices as fire risk indicators in savanna ecosystems," *IEEE Trans. Geosci. Remote Sens.*, vol. 44, no. 6, pp. 1622–1632, Jun. 2006.

[83] F. Bovolo and L. Bruzzone, "A split-based approach to unsupervised change detection in large-size multitemporal images: Application to tsunami-damage assessment," *IEEE Trans. Geosci. Remote Sens.*, vol. 45, no. 6, pp. 1658–1670, Jun. 2007.

[84] L. Bruzzone and F. Bovolo, "A conceptual framework for change detection in very high geometrical resolution remote sensing images," in *Proc. IEEE Int. Geosci. Remote Sens. Symp.*, Honolulu, HI, 2010, pp. 2555–2558.

[85] F. Bovolo, S. Marchesi, and L. Bruzzone, "A nearly lossless 2D representation and characterization of change detection information in multispectral images," in *Proc. IEEE Int. Geosci. Remote Sens. Symp.*, Honolulu, HI, 2010, pp. 3074–3077.

[86] V. J. D. Tsai, "A comparative study on shadow compensation of color aerial images in invariant color models," *IEEE Trans. Geosci. Remote Sens.*, vol. 44, no. 6, pp. 1661–1671, Jun. 2006.

[87] R. A. Schowengerdt, *Remote Sensing: Models and Methods for Image Processing*, 2nd. San Diego, CA: Academic, 1997.

[88] J. Inglada and J. Michel, "Qualitative spatial reasoning for high-resolution remote sensing image analysis," *IEEE Trans. Geosci. Remote Sens.*, vol. 47, no. 2, pp. 599–612, Feb. 2009.

[89] A. Ferro, D. Brunner, and L. Bruzzone, "An advanced technique for building detection in VHR SAR images," *Proc. SPIE Image Signal Process. Remote Sens. XV*, vol. 7477, 2009. DOI: 10.1117/12.830719.

[90] ENVIITT visual information solutions, [Online]. Available: www.ittvis.com

[91] P. L. Rosin and E. Ioannidis, "Evaluation of global image thresholding for change detection," *Pattern Recognit. Lett.*, vol. 24, no. 14, pp. 2345–2356, 2003.

[92] A. P. Dempster, N. M. Laird, and D. B. Rubin, "Maximum likelihood from incomplete data via the EM algorithm," *J. Roy. Stat. Soc.*, vol. 39, no. 1, pp. 1–38, 1977.

[93] T. K. Moon, "The expectation-maximization algorithm," *Signal Process. Mag.*, vol. 13, no. 6, pp. 47–60, 1996.

[94] eCognition by Trimble GeoSpatial, Trappentreustr. 1, Munich, Germany, 2004. [Online]. Available: http://www.ecognition.com/

ABOUT THE AUTHORS

Lorenzo Bruzzone (Fellow, IEEE) received the laurea (M.S.) degree in electronic engineering *(summa cum laude)* and the Ph.D. degree in telecommunications from the University of Genoa, Genoa, Italy, in 1993 and 1998, respectively.

He is currently a Full Professor of Telecommunications at the University of Trento, Povo, Trento, Italy, where he teaches remote sensing, radar, pattern recognition, and electrical communications. He is the Founder and the Director of the Remote Sensing Laboratory, Department of Information Engineering and Computer Science, University of Trento. His current research interests are in the areas of remote sensing, radar and SAR, signal processing, and pattern recognition. He promotes and supervises research on these topics within the frameworks of more than 28 national and international projects. He is the author (or coauthor) of 114 scientific publications in referred international journals (76 in IEEE journals), more than 170 papers in conference proceedings, and 16 book chapters. He is editor/coeditor of ten books/conference proceedings and one scientific book. He has served on the scientific committees of several international conferences and was invited as keynote speaker in more than 20 international conferences and workshops. He is a member of the Managing Committee of the Italian Inter-University Consortium on Telecommunications. Since 2009 he is a member of the Administrative Committee of the IEEE Geoscience and Remote Sensing Society.

Dr. Bruzzone ranked first place in the Student Prize Paper Competition of the 1998 IEEE International Geoscience and Remote Sensing Symposium (Seattle, WA, July 1998). He was a recipient of the Recognition of the IEEE Transactions on Geoscience and Remote Sensing Best Reviewers in 1999 and was a Guest Co-Editor of different special issues of international journals. In the past years, joint papers presented by his students at international symposia and master theses that he supervised have received international and national awards. He was the General Chair/Co-Chair of the 1st, 2nd, and 6th IEEE International Workshop on the Analysis of Multi-Temporal Remote-Sensing Images (MultiTemp), and is currently a member of the Permanent Steering Committee of this series of workshops. Since 2003, he has been the Chair of the SPIE Conference on Image and Signal Processing for Remote Sensing. From 2004 to 2006, he served as an Associated Editor of the IEEE Geoscience and Remote Sensing Letters, and currently is an Associate Editor for the IEEE Transactions on Geoscience and Remote Sensing and the *Canadian Journal of Remote Sensing*. Since April 2010, he has been the Editor of the IEEE Geoscience and Remote Sensing Newsletter. In 2008 he was appointed as a member of the joint NASA/ESA Science Definition Team for the radar instruments for *Outer Planet Flagship Missions*. In 2012, he was appointed *Distinguished Speaker* of the IEEE Geoscience and Remote Sensing Society. He is a member of the Italian Association for Remote Sensing (AIT).

Francesca Bovolo (Member, IEEE) received the "Laurea" (B.S.) and "Laurea Specialistica" (M.S.) degrees in telecommunication engineering *(summa cum laude)* and the Ph.D. degree in communication and information technologies from the University of Trento, Povo, Trento, Italy, in 2001, 2003, and 2006, respectively.

She is presently a Research Fellow at the Remote Sensing Laboratory, Department of Information Engineering and Computer Science, University of Trento. Her main research activity is in the area of remote sensing image processing. In particular, her interests are related to multitemporal remote sensing image analysis and change detection in multispectral and SAR images, and very-high-resolution images. She conducts research on these topics within the frameworks of several national and international projects.

Dr. Bovolo is a referee for the IEEE Transaction on Geoscience and Remote Sensing, the IEEE Geoscience and Remote Sensing Letters, the IEEE Transactions on Image Processing, the IEEE Journal of Selected Topics in Applied Earth Observations and Remote Sensing, the *International Journal of Remote Sensing*, *Pattern Recognition*, *Pattern Recognition Letters*, *Remote Sensing of Environment*, *Photogrammetric Engineering and Remote Sensing*, *Photogrammetry and Remote Sensing*, the IEEE Transactions on Aerospace and Electronic Systems, and *Sensors*. She ranked first place in the Student Prize Paper Competition of the 2006 IEEE International Geoscience and Remote Sensing Symposium (Denver, CO, August 2006). Since January 2011, she has been an Associate Editor of the IEEE Journal of Selected Topics in Applied Earth Observations and Remote Sensing. She is the Guest Editor of the Special Issue on "Analysis of Multitemporal Remote Sensing Data" of the IEEE Transaction on Geoscience and Remote Sensing. She is the Technical Chair of the 6th International Workshop on the Analysis of Multi-Temporal Remote-Sensing Images (MultiTemp 2011). Since 2006, she has served on the Scientific Committee of the SPIE International Conference on "Signal and Image Processing for Remote Sensing." She has served on the scientific committee of the IEEE 4th and 5th International Workshop on the Analysis of Multi-Temporal Remote Sensing Images (MultiTemp 2007 and 2009).